P-05-20

# Oskarshamn site investigation

# Combined interference test and tracer test between KLX02 and HLX10

Erik Gustafsson, Jan-Erik Ludvigson
Geosigma AB

February 2005

**Svensk Kärnbränslehantering AB**
Swedish Nuclear Fuel
and Waste Management Co
Box 5864
SE-102 40 Stockholm Sweden
Tel 08-459 84 00
+46 8 459 84 00
Fax 08-661 57 19
+46 8 661 57 19

ISSN 1651-4416
SKB P-05-20

# Oskarshamn site investigation

# Combined interference test and tracer test between KLX02 and HLX10

Erik Gustafsson, Jan-Erik Ludvigson
Geosigma AB

February 2005

*Keywords:* Tracer test, Interference test, Pumping test.

# Abstract

This report describes the performance, evaluation and interpretation of a combined pumping and tracer test at Laxemar, Oskarshamn. The objectives of the activity were to assess the connectivity between boreholes KLX02 and HLX10 through potential fracture zones intersecting both boreholes and to determine the hydraulic properties for the pumping hole HLX10 as well as the monitored responses in KLX02 and other boreholes responding in the area. The tracer test also provided an opportunity to determine transport properties of the flow paths involved, in the case of a tracer breakthrough.

The test did not give any breakthrough of tracer over the 260 m distance between the boreholes but good hydraulic responses was monitored and quantitative evaluation of hydraulic parameters could be made. The main reason for the lack of tracer breakthrough is probably a combination of more complicated flow geometry (no direct contact) and the fact that the pumping was stopped after about a week due to power failure and then re-started after a week.

# Sammanfattning

Denna rapport beskriver genomförandet, utvärderingen samt tolkningen av ett kombinerat pump- och spårförförsök i Laxemar, Oskarshamn. Syftet med aktiviteten var dels att studera konnektionen mellan borrhålen KLX02 och HLX10 via potentiella sprickzoner som skär de två borrhålen samt att utvärdera hydrauliska egenskaper för pumphålet HLX10 samt de med KLX02 konnekterade flödesvägarna/sprickzonerna. Spårförsöket gav också en möjlighet att bestämma transportegenskaper för flödesvägarna i det fall ett genombrott skulle detekteras.

Testet gav inget spårämnesgenombrott för den 260 m långa flödesvägen men goda hydrauliska responser gjorde det möjligt att kvantifiera hydrauliska parametrar. Anledningen till att inget spårämnesgenombrott erhölls bedöms vara en kombination av en komplicerad flödesgeometri (ingen direktkontakt) samt att pumpningen avbröts efter en vecka pga. strömavbrott/haveri för att sedan återupptas en vecka senare.

# Contents

# 1 Introduction

This document reports the results gained by the combined interference test and tracer test between KLX02 and HLX10, which is one of the activities performed within the site investigation at Oskarshamn. The work was carried out in accordance with activity plan AP PO 400-04-62. In Table 1-1 controlling documents for performing this activity are listed. Both activity plan and method descriptions are SKB's internal controlling documents.

**Table 1-1. Controlling documents for the performance of the activity.**

| **Activity plan** | **Number** | **Version** |
|---|---|---|
| Kombinerat pumptest och spårförsök mellan borrhål KLX02 och HLX10 | AP PF 400-04-62 | 1.0 |
| **Method descriptions** | **Number** | **Version** |
| Metodbeskrivning för flerhålsförsök | SKB MD 540.004 | 1.0 |
| Metodinstruktion för analys av injektions- och enhålspumptester | SKB MD 320.004 | 1.0 |
| Metodbeskrivning för interferenstester | SKB MD 330.003 | 1.0 |

During drilling of core borehole KLX04, water used as drilling fluid has been pumped from borehole HLX10 at Laxemar, see Figure 1-1. HLX10 is located about 250 m (at the surface) from borehole KLX02, situated north of HLX10.

During drilling of KLX04, the pumping in HLX10 for drilling fluid caused pressure disturbances that could be monitored in KLX02 as good and fast pressure responses as shown in Figure 1-2. The co-variation between the boreholes is obvious even though the magnitude is much smaller in KLX02. One hypothesis was that a fractured and highly conductive part of KLX02 at about 250 m borehole length is in direct hydraulic contact with HLX10.

In order to test this hypothesis, a combined pumping test and tracer test was performed.

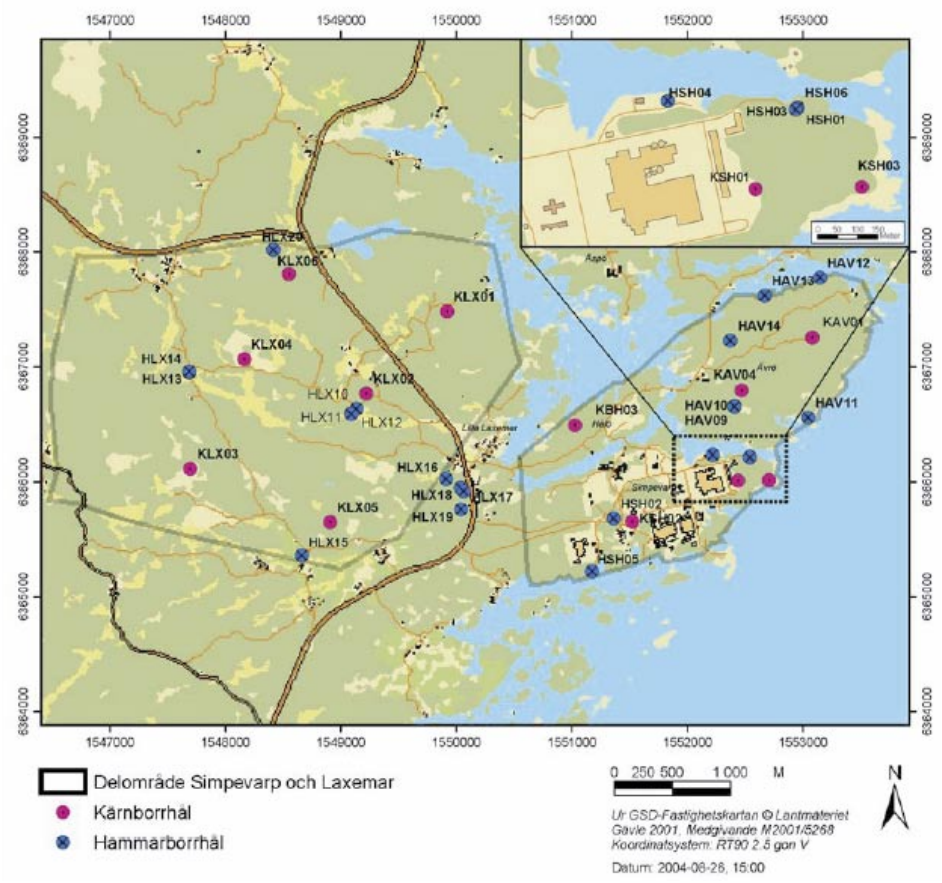


***Figure 1-1.*** *Overview of the Oskarshamn site investigation area, including boreholes.*

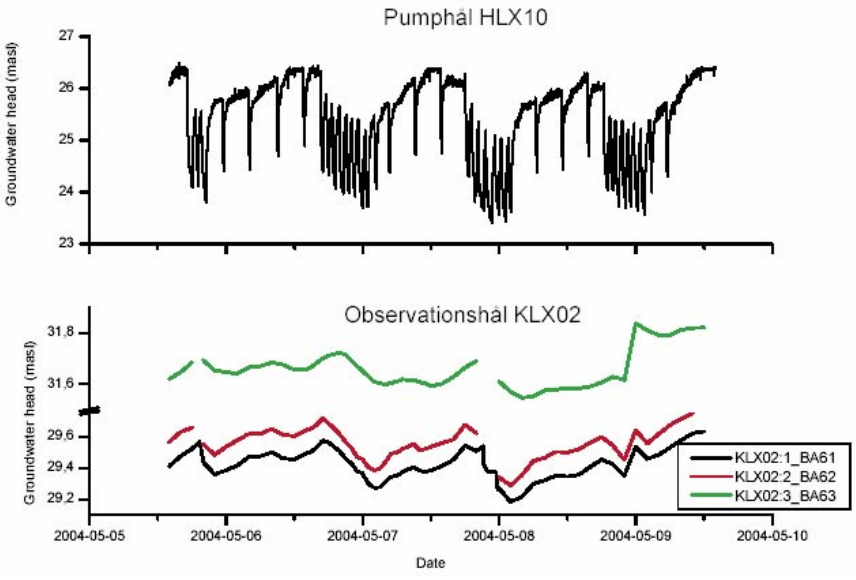


***Figure 1-2.*** *Groundwater head (m.a.s.l) in pumping hole HLX10 (upper graph) and in three sections of KLX02 (lower graph).*

**Table 1-2. Data references.**

| Subactivity | Database | Identity number |
|---|---|---|
| Pumping and interference test between KLX02 and HLX10 | SICADA | Field note 534 |

# 2 Objective and scope

The objectives of the activity are:

- To assess the connectivity between boreholes KLX02 and HLX10 through potential fracture zones intersecting both boreholes
- To determine the hydraulic properties for the pumping hole HLX10 as well as the monitored responses in KLX02 and other boreholes responding in the area.

The tracer test also provided an opportunity to determine transport properties of the flow paths involved, in the case of a tracer breakthrough.

This report describes the field performance, evaluation and interpretation of the combined pumping test and tracer test performed in July 2004.

# 3 Equipment

## 3.1 Description of equipment

Pumping was performed in HLX10 using the down-hole pump previously used for the pumping of drilling water to KLX04.

Borehole KLX02 was instrumented with a double-packer system dividing the borehole in three intervals:

Section 1: 256.4–1,700 m (KLX02:1).

Section 2: 207.9–255.4 m (KLX02:2).

Section 3: 0–206.9 m (KLX02:3).

No packers were installed in HLX10. Pressure transducers were installed in the pumping well HLX10 and in the three sections of KLX02.

Borehole HLX11, located about 50 m from the pumping well, also had pressure registration as a part of the ordinary monitoring system (HMS).

All pressure registration data were recorded by the DMS/HMS system.

Tracer solution (Rhodamine WT) was added to KLX02:2 through the pressure monitoring line by removing the pressure transducer during the injection procedure. The injection was done by means of a Micropump gear pump.

# 4 Execution

## 4.1 General

The methods together with the nomenclature and symbols used for the evaluation of the combined pumping and tracer test between boreholes KLX02 and HLX10 are according to the Instruction for analysis of single-hole injection- and pumping tests (SKB MD 320.004, Version 1.0) and the methodology description for interference tests (SKB MD 330.003, Version 1.0). Additional symbols used are explained in the text.

## 4.2 Preparations

The instrumentation of the pumping well, HLX10, with pressure transducers and downhole pump was done for drilling purposes several months in advance of the test and no new calibration of the flow meter was done. The pressure transducers in HLX10, HLX11 and KLX02 were calibrated with manual levelling after the test had been finalized.

1,000 litres of water was pumped from HLX10 into a storage tank one week prior to the test start to be used for tracer injection.

## 4.3 Execution of field work

The field work was performed during a three-week period in July 2004. The following test sequence was used:

**Day 1** (6 July 2004)

- Start pumping in HLX10 (flow rate c 71 L/min).
- Control of pumping and pressure responses through HMS.
- Start sampling of pumped water from HLX10, 2 samples/day (containing 8 ml) for tracer analysis. One sample every day for analysis of electrical conductivity.

**Day 2** (7 July 2004)

- Deflation and demobilisation of mini-packer and pressure transducer in KLX02, section 2. Mounting of injection hose and re-installation of mini-packer.
- Start injection of tracer solution (Rhodamine WT, 1,000 ppm) in KLX02, section 2.
- Sampling of pumped water from HLX10, as above.
- Control of pumping and pressure responses through HMS.

**Day 3** (8 July 2004)

- Stop injection of tracer solution (Rhodamine WT, 1,000 ppm). In total 200 litres injected.
- Start injection of flushing water in KLX02, section 2 (unlabelled water pumped from HLX10 prior to test start).
- Sampling of pumped water from HLX10, as above
- Control of pumping and pressure responses through HMS.

**Day 4–6** (9–11 July 2004)

- Ongoing injection of flushing water in KLX02, section 2.
- Sampling as above.
- Control of pumping and pressure responses through HMS.

**Day 7** (12 July 2004)

- Stop injection of flushing water in KLX02, section 2. In total 1,000 litres injected.
- Re-installation of pressure transducer in KLX02, section 2.
- Sampling as above.
- Control of pumping and pressure responses through HMS.

**Day 8–14** (13–19 July 2004)

- No pumping in HLX10, due to electric distribution box hit by lightning.
- Sampling as above.
- Control of pressure responses through HMS.

**Day 15** (20 July 2004)

- Restart of pumping in HLX10.
- Sampling as above.
- Control of pressure responses through HMS.

**Day 16–20** (21–25 July 2004)

- Pumping in HLX10.
- Sampling as above.
- Control of pressure responses through HMS.

**Day 21** (26 July 2004)

- Final sampling in HLX10.

**Day 22** (27 July 2004)

- Stop of pumping in HLX10.

## 4.4 Data handling/post processing

Tracer and electrical conductivity samples were analysed at the Geosigma Laboratory in Uppsala. The analyses revealed no breakthrough of tracer during the time of pumping.

Pump flow and pressure data were monitored by the HMS system. Further data processing was made with the SKB software PUMPKONV and the commercial software AQTESOLV.

## 4.5 Analyses and interpretations

Firstly, a qualitative evaluation was performed to identify the actual flow regimes during the flow- and recovery period (e.g. wellbore storage, pseudo-radial flow, pseudo-spherical flow etc) and possible outer hydraulic boundary conditions. The analysis of flow regimes was made from the pressure responses together with the corresponding pressure derivatives versus time, preferably in the log-log diagrams. In addition, a simple response analysis of the hydraulic connections between the pumping borehole HLX10 and the responding observation sections in borehole HLX11 and KLX02 according to the methodology description for interference tests was made prior to the quantitative hydraulic analysis.

The quantitative, transient interpretation of hydraulic parameters from the pumping borehole (e.g. transmissivity and skin factor) and from the observation sections (transmissivity, storativity) was mainly based on the identified pseudo-radial flow regimes in an equivalent porous medium. Finally, a steady-state analysis from the flow period (Moye's formula) was also made for the pumping borehole.

The software AQTESOLV was used for the transient evaluation. A brief description of the software and its application is provided in related pumping test reports from HTHB tests. For the actual test the Dougherty-Babu model, accounting for wellbore storage and skin effects, was used for the analysis of the pumping borehole, HLX10. For the observation sections, the model by Hantush-Jacob was used. This model accounts for leakage support from adjacent structures in the rock.

No corrections of the measured data, e.g. for changes of the barometric pressure, tidal fluctuations or natural trends due to precipitation etc have been made by the analysis.

## 4.6 Nonconformities

The observation hole HLX11 used for this activity was previously, and at the time when the field activity was performed, named and assumed to be HLX12. However, later findings showed that the boreholes had been mixed up and what we had been informed was HLX12 was in fact HLX11. The boreholes are located only about 5 m from each other.

An analysis of the significance of the mix up on parameter values was made taken into account that the distance from the pumping well decreased by a maximum of 25 m in the lower interval HLX11:1. The distance to the upper interval HLX11:2 is the same as to HLX12:2. The analysis is very much influenced by the chosen point of application in the borehole. The correct point of application would be the location of the water conducting structure in the borehole. This is however not known as no measurements to assess this have been made in HLX 11. Hence, by choosing the point of application to be 22 m in HLX11 this would yield the same distance to the pumping well as the analysis is based on.

# 5 Results of tracer pumping test in HLX10

This chapter only deals with pressure responses as no tracer breakthrough was observed in HLX10.

Test data diagrams with pressure and pressure derivative during the flow- and recovery period together with the simulated response curves are presented in Appendix 1. The same simulated response curves for pressure and pressure derivative are shown in both log-log and lin-log diagrams (no separate analyses were made in these types of diagrams).

## 5.1 Response analysis of the observation borehole sections

### 5.1.1 Overview of responses

As can be seen from Figures A-3–6 in Appendix 1, the responses in the pumping borehole HLX10 were heavily influenced by precipitation during the later part of both the flow- and recovery period of the pumping test. Also the responses in the observation borehole sections in KLX02 (Figures A-11–12) and HLX11 (Figures A-25–26) were affected by the precipitation. The pressure in all these sections started to increase as an effect of the rainfall starting at c 17.00 hours on the 9th of July. The response analysis was therefore performed on the first part of the flow period before this time.

In Table 5-1, the geometrical distances to the observation sections from the pumping borehole HLX10 are shown. The distances are calculated as the shortest distance between the points of application in the borehole sections. Since no information of e.g. inflow zones is available in the percussion boreholes HLX10 and HLX11 the points of application in these boreholes were assumed, see also Chapter 4.6. In KLX02, the points of application were estimated from the location of inflow zones, identified from the previous difference flow logging in this borehole /Rouhiainen P, 2000/ together with a correlation study between difference flow logging, borehole-TV and –radar images /Carlsten et al. 2001/.

The maximal drawdown $s_p$ in the observation sections before the rainfall on the 9th of July is shown in Table 5-1. The pressure registration in section KLX02:2 was terminated after c 1 day due to injection of tracer in this section. Before this time, the pressure drawdown behaviour in this section was very similar to the drawdown behaviour in section KLX02:1. In the response analysis, it was assumed that the same drawdown as in this section would have been measured at the actual time, 9th July, chosen for this analysis. Finally, the time lags to achieve a drawdown of 0.1 m, $dt_L[s = 0.1\ m]$, in the observation sections are listed in Table 5-1.

**Table 5-1. Geometrical distances between the points of application in the pumping borehole HLX10 and the observation sections in borehole HLX11 and KLX02 together with the maximal drawdown and response time lags for the sections.**

| Pumping borehole | Observation borehole | Section (m) | Label | Hydr. p.a. (m) | $r_s$ (m) | $s_p$ (m) | $dt_L$[s = 0.1 m] (min) |
|---|---|---|---|---|---|---|---|
| HLX10 | | 0–85 | | 85 | 0 | 4.2 | – |
| | HLX11 | 0–13 | HLX11:2 | 7 | 90 | 2.4 | 140 |
| | HLX11 | 14–70 | HLX11:1 | 22 | 76 | 2.3 | 42 |
| | KLX02 | 0–206.9 | KLX02:3 | 100 | 190 | 1.4 | 280 |
| | KLX02 | 207.9–255.4 | KLX02:2 | 250 | 260 | (1.9)* | 68 |
| | KLX02 | 256.4–1,700 | KLX02:1 | 317 | 310 | 1.9 | 72 |

* the pressure registration in this section was terminated after c 1 day of pumping due to tracer injection

### 5.1.2 Response analysis

The response time lags ($dt_L$) in the observation sections during the tracer pumping test in HLX10 are shown in Table 5-1. The time lags were in this case derived from the drawdown curves in the observation borehole sections at a drawdown of 0.1 m.

The normalised response time $dt_L$[s = 0.1 m] / $r_s^2$ with respect to the distance to the pumping borehole (Index 1) was firstly calculated. The normalised response time is inversely related to the hydraulic diffusivity (T/S) of the formation, i.e. the shorter the response time the higher the hydraulic diffusivity. The distances to the borehole sections are shown in Table 5-1. In addition, the normalized drawdown $s_p/Q_p$ with respect to the flow rate (Index 2) was calculated. The final flow rate $Q_p$ during the tracer pumping test was c 71 L/min. In Figure 5-1, the normalized drawdown is plotted versus the normalized response time for the responding observation sections. The drawdown in section KLX02:2 is uncertain.

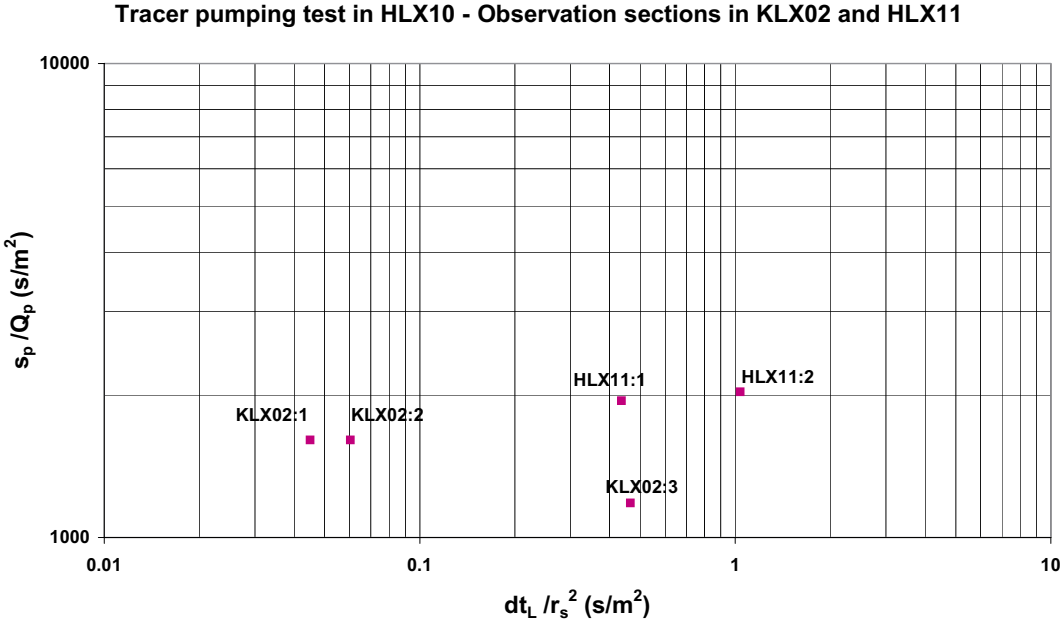


***Figure 5-1.*** *Normalized drawdown versus normalized response times for the responding observation sections during the tracer pumping test in HLX10.*

Figure 5-1 shows that the normalised response times for the sections KLX02:1 and KLX02:2 are significantly lower than for the other observation sections. This fact indicates that these sections are better hydraulically connected to the pumping borehole HLX10. The response in section KLX02:2 is however uncertain as discussed above. The responses in HLX11 and in section KLX02:3 are more delayed which may indicate that these sections are not located within the same fracture zone as the previous sections in KLX02 or alternatively, are only weakly (indirectly) hydraulically connected to the zone.

### 5.1.3 Possible interpretation of the fracture zone geometry

To study the possible fracture zone geometry between the responding boreholes during the tracer pumping test, 3D pictures were prepared for the actual boreholes, see Figure 5-2 and 5-3. The seismic reflector A, described in /Ekman, 2001/, is shown in the figures. Furthermore, the four most conductive fractures identified from the difference flow logging in KLX02 /Rouhiainen, 2000/ are shown. The planes of the identified most conductive fractures in KLX02 were extrapolated to their possible intersections with the other boreholes. Figure 5-2 shows the seismic reflector A and the extrapolated plane of fracture 4, intersecting KLX02 at c 317 m together with the packer positions in the boreholes. All extrapolated fracture planes (1–4) are indicated in Figure 5-3.

The interpreted orientation of reflector A and of the four most conductive fractures (1–4) in KLX02 from the correlation study described above together with the borehole intersections are presented in Table 5-2. In addition, the estimated transmissivities of the conductive fractures from the difference flow logging are presented in the table.

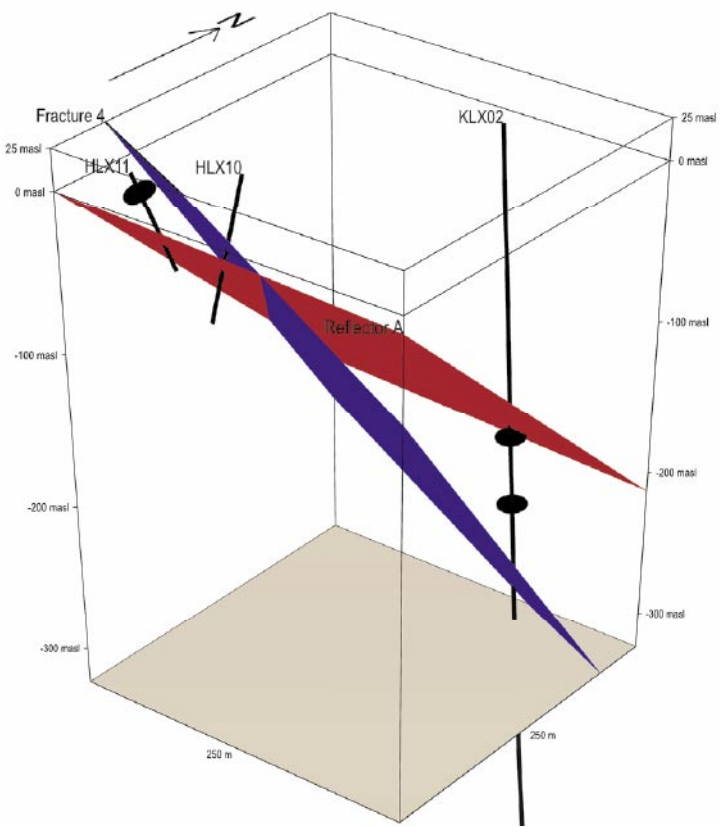


***Figure 5-2.*** *3D-picture of the seismic reflector A (red) and possible geometrical interpretation of fracture 4 (blue) between boreholes HLX10, HLX11 and KLX02 according to Table 5-2.*

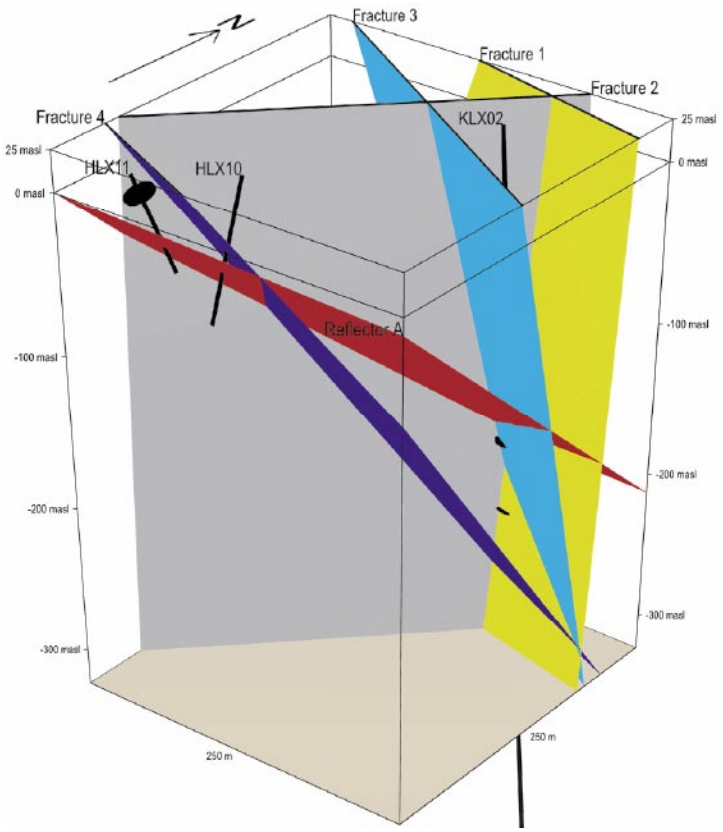


***Figure 5-3.*** *3D-picture of possible geometrical interpretation of fractures 1–4 between boreholes HLX10, HLX11 and KLX02 according to Table 5-2.*

**Table 5-2. Orientation of the seismic reflector A together with the BIPS-orientations of the most conductive fractures (1–4) in KLX02 and the borehole intersections with the extrapolated planes of these fractures together with their estimated transmissivity from the difference flow logging.**

| Reflector/ conductive fracture | Orientation Strike/dip | Borehole intersection (m) | Extrapolated intersection (m) | | Transmissivity** ($m^2/s$) |
|---|---|---|---|---|---|
| | | | HLX10 | HLX11 | |
| A | 273/39 | KLX02:c 200 | 55 | 52 | – |
| 1 | 104/85 | KLX02:213.3 | No | No | $1.9\times10^{-6}$ |
| 2 | 045/89 | KLX02:251.3 | No | No | $5.5\times10^{-6}$*** |
| 3 | 302/78 | KLX02:251.6 | No | No | $1.4\times10^{-6}$ |
| 4 | 295/54 | KLX02:317.1 | 43 | c –10* | $5.5\times10^{-6}$*** |

* the extrapolated fracture plane does not intersect HLX11 but is sub-parallel and as closest about 10 m from the top of the borehole
** transmissivity estimated from difference flow logging
*** determined at flow rates close to the upper measurement limit for flow rate

Table 5-2 shows that only reflector A is assumed to intersect all three boreholes. By the design of the tracer test, it was assumed that the pumped fracture zone intersecting HLX10 would intersect KLX02 at c 250 m, possibly at the conductive fractures 2–3 at c 251 m. However, the observed response pattern during the tracer pumping test seems not to support such a geometrical interpretation, cf Table 5-1.

According to the BIPS-interpretations in Table 5-2, fractures 2 and 3 (and also fracture 1) in KLX02 are steeply dipping and may therefore not intersect the other boreholes, cf Figure 5-3. Fracture 4 is more gently dipping and intersects HLX10 at c 43 m according to Table 5-2. The extrapolated plane of fracture 4 does not intersect HLX11 but is sub-parallel and as closest c 10 m from the top of HLX11, see Figure 5-2. However, if the dip of the zone is assumed to be a few degrees less that that in Table 5-2, it will then intersect the upper part of HLX11.

A possible interpretation of the responses during the tracer pumping test in HLX10 may thus be that fracture 4, intersecting the pumping borehole HLX10 at c 43 m and the observation borehole section KLX02:1 at c 317 m, is the main hydraulic conductor between the boreholes. Such an interpretation is supported by the response diagram in Figure 5-1. The assumed response in section KLX02:2 may possibly have been indirectly transmitted along fractures 2 or 3, cf Figure 5-3, or via other connecting fractures to fracture 4.

## 5.2 Evaluation of hydraulic parameters

In Table 5-3 the estimated specific capacity of the pumping borehole HLX10 is presented together with the estimated cumulative transmissivity of the two lower observation sections in KLX02 from the previous sequential difference flow logging in 3 m sections /Rouhiainen, 2000/. The upper section in KLX02 is cased to 202.95 m /Ekman, 2001/ and no conductive fractures were identified in the open part of the section during the difference flow logging. No further hydraulic information is available from the percussion boreholes HLX10 and HLX11.

**Table 5-3. Specific capacity in the pumping borehole HLX10 together with cumulative transmissivity ($\Sigma T_D$) in the observation sections in borehole KLX02 from the previous difference flow logging.**

| Pumping borehole | Section (m) | $Q_p/s_p$* ($m^2/s$) | Observation borehole section | Section (m) | $\Sigma T_D$ ($m^2/s$) |
|---|---|---|---|---|---|
| HLX10 | 0–85 | $2.8\times10^{-4}$ | | | – |
| | | | HLX11:2 | 0–13 | – |
| | | | HLX11:1 | 14–70 | – |
| | | | KLX02:3 | 0–206.9 | $<3\times10^{-9}$** |
| | | | KLX02:2 | 207.9–255.4 | $2.3\times10^{-5}$ |
| | | | KLX02:1 | 256.4–1,700 | $1.0\times10^{-5}$ |

* based on the maximal drawdown before the rainfall at c 17.00 hours on the 9th of July
** borehole KLX02 is cased to 202.95 m

### 5.2.1 Pumping borehole HLX10

#### *Comments to the test*

The test was performed as a constant-flow rate pumping test. The flow rate was c 71 L/min during the entire flow period, see Figure A-1 in Appendix 1. The changes of the atmospheric pressure together with the precipitation during the entire test period are shown in Figure A-2 and A-3, respectively. The pressure history is shown in Figure A-4.

The total duration of the flow period was c 7 days but natural pressure variations, e.g. due to precipitation, started to influence the drawdown behaviour in HLX10 already after c 17 hours, see Figure A-3. The pressure increased during the rainfall, starting at c 17:00 hours on the 9th of July. The maximal drawdown in HLX10 (before the rainfall) was c 4.2 m. The pressure recovery was measured for c 3.5 days but the heavy rainfall on the 13th of July also distorted the recovery period.

#### *Interpreted flow regimes*

To facilitate the influence of the rainfall, the precipitation is shown separately in lin-log diagrams for the flow- and recovery period in Figures A-5 and 6, respectively. Test diagrams in lin-log and log-log diagrams during the flow- and recovery period for HLX10 are presented in Figures A-7–10 in Appendix 1. During the flow period, a rather well-defined pseudo-radial flow regime is indicated during the first c 1,000 min. During this time period, no precipitation was registered, cf Figure A-5. After this time, the pressure is affected by natural fluctuations and rainfall.

The recovery period was also disturbed by precipitation which makes interpretation of flow regimes difficult.

#### *Interpreted parameters*

The transient interpretation of the flow period of the test is shown in log-log and lin-log diagrams in Figures A-7–8. An approximate analysis was also made from the recovery period with similar results. The results are shown in Table 5-4. The most representative hydraulic parameter estimation is chosen from the interpretation of the flow period due to a much longer and more well-defined pseudo-radial flow regime during this period.

### 5.2.2 Observation section KLX02:1 (256.4–1,700 m)

#### *Comments to the test*

The response analysis in Figure 5-1 indicates a direct response in section KLX02:1, probably along the same fracture zone as intersected by the pumping borehole HLX10. Figure 5-2 suggests that the response was transmitted along fracture (zone) 4, intersecting KLX02 at c 317 m, cf Table 5-2.

The pressure history in the observation sections in KLX02 during the entire test period together with the precipitation during the period is shown in Figure A-11 and -12, respectively. As in borehole HLX10, the pressure was strongly influenced by the rainfall periods. The pressure started to increase c 17:00 on the 9th of July during the flow period due to precipitation. The maximal drawdown in section KLX02:1 (before the rainfall) was c 1.9 m. The pressure recovery seems slightly less influenced by precipitation than during the flow period.

#### *Interpreted flow regimes*

Test diagrams in lin-log and log-log diagrams for section KLX02:1 during the flow- and recovery period are presented in Figures A-13–16 in Appendix 1. During the flow period, a rather well-defined pseudo-radial flow regime is indicated between c 500–3,000 min. During this time period, only small amounts of precipitation was registered, cf Figure A-5. After this time, the pressure was affected by the rainfall.

During the recovery period, a pseudo-radial flow regime is also indicated at similar (equivalent) time interval. Only small amounts of precipitation was registered during this time interval, cf Figure A-6. After this time, the pressure was more affected by precipitation.

#### *Interpreted parameters*

The transient interpretation of the flow- and recovery period of the test is shown in log-log and lin-log diagrams in Figures A-13–16. The interpretation is based on the time intervals before the rainfall which occurred by the end of both the flow-and recovery period. A slight leakage support from precipitation was observed during these time intervals as reflected by the parameter r/B in the analysis. The results of the interpretation of hydraulic parameters from section KLX02:1 are shown in Table 5-5. Although the results are very similar from the flow- and recovery period, respectively, the most representative hydraulic parameter estimation is chosen from the flow period.

### 5.2.3 Observation section KLX02:2 (207.9–255.4 m)

#### *Comments to the test*

The response analysis in Figure 5-1, based on the shortened registration in KLX02:2, also indicates a direct response for this section. The response may have been partly transmitted along the same fracture zone as intersected by the pumping borehole HLX10, i.e. along fracture (zone) 4. Since this fracture (zone) does not intersect section KLX02:2 according to Figure 5-2, the response may have been transmitted to this section via other fractures, e.g. fracture 2 in Figure 5-3. Alternatively, sections KLX02:1 and :2 may be hydraulically short-circuited by local fractures close to the packer.

The pressure history in the observation sections in KLX02 during the entire test period together with the precipitation during the period is shown in Figure A-11 and -12, respectively. The registration in section KLX02:2 were terminated after c 1 day due to tracer injection in this section. The pressure transducer was re-installed after tracer injection. However, at a shallower depth below ground surface, which was due to high friction in the stand pipe. As in section KLX02:1, the pressure was influenced by the rainfall periods. The pressure started to increase at c 17:00 hours on the 9$^{th}$ of July during the flow period due to precipitation. The maximal drawdown in section KLX02:2 (before stop of registration) was c 1.2 m. The pressure recovery seems slightly less influenced by precipitation than during the flow period.

#### *Interpreted flow regimes*

Test diagrams in lin-log and log-log diagrams for section KLX02:2 during the flow- and recovery period are presented in Figures A-17–20 in Appendix. During the short flow period, a pseudo-radial flow regime is indicated between c 500–1,200 min. During this time period, only small amounts of precipitation was registered, cf Figure A-5.

During the recovery period, a pseudo-radial flow regime is also indicated during the (equivalent) time interval 500–2,000 min. Only small amounts of precipitation was registered during this time interval, cf Figure A-6. After this time, the pressure was more affected by precipitation.

#### *Interpreted parameters*

The transient interpretation of the flow- and recovery period of the test is shown in log-log and lin-log diagrams in Figures A-17–20. The interpretation is based on the time intervals before the rainfall which occurred by the end of both the flow-and recovery period. A slight leakage support from precipitation was observed during these time intervals as reflected by the parameter r/B in the analysis. The results of the interpretation of hydraulic parameters from section KLX02:2 are shown in Table 5-5. Although the results are very similar from the flow- and recovery period, respectively, the most representative hydraulic parameter estimation is chosen from the recovery period in this case due to the limited registration in this section during the flow period.

### 5.2.4 Observation section KLX02:3 (0–206.9 m)

#### *Comments to the test*

The response analysis in Figure 5-1 indicates a weak and delayed response in this section, indicating that the section is not located in the same fracture zone as intersected by the pumping borehole HLX10, i.e. along fracture (zone) 4. Furthermore, Figure 5-3 indicates that none of the depicted fracture (zones) penetrates this section. This is consistent with the information in Table 5-3. The response may have been transmitted indirectly via local fractures. Alternatively, sections KLX02:2 and :3 may be hydraulically short-circuited by local fractures close to the packer.

The pressure history in the observation sections in KLX02 during the entire test period together with the precipitation during the period is shown in Figure A-11 and -12, respectively. As in section KLX02:1, the pressure in section KLX02:3 was influenced by the rainfall periods. The pressure started to increase at c 17:00 hours on the 9$^{th}$ of July during the flow period due to precipitation. The maximal drawdown in section KLX02:3 (before the rainfall) was c 1.4 m. The pressure recovery seems slightly less influenced by precipitation than during the flow period.

#### *Interpreted flow regimes*

Test diagrams in lin-log and log-log diagrams for section KLX02:3 during the flow- and recovery period are presented in Figures A-21–24 in Appendix. No well-defined pseudo-radial flow regime occurred during the flow period. The response seems to be dominated by leakage support from the precipitation. A short period of apparent pseudo-radial flow is indicated between 1,000–2,000 min. However, this period probably do not represent the hydraulic properties of this section. The response during the recovery period is similar to that during the flow period. No pseudo-radial flow regime occurred during recovery.

#### *Interpreted parameters*

An attempt to transient interpretation of the flow- and recovery period of the test was made as shown in log-log and lin-log diagrams in Figures A-21–24. However, this interpretation is not considered as representative for the hydraulic properties of the section. The response analysis in Figure 5-1 indicated that the section most likely is indirectly connected to the pumping borehole HLX10. This fact is further supported by the high calculated values on the storativity for this section. The response in KLX02:3 seem to be strongly influenced by leakage support from precipitation as reflected by the apparent high value on the leakage factor r/B in the analysis. Therefore, the results of the interpretation of hydraulic parameters from section KLX02:3 are shown within brackets in Table 5-5.

### 5.2.5 Observation sections HLX11:1 (14–70 m) and HLX11:2 (0–13 m)

#### *Comments to the test*

The response analysis in Figure 5-1 together with the 3D-picture of assumed fracture zones in Figure 5-3 indicate a weak and delayed response in both these sections, indicating that none of the sections is located in the same fracture zone as intersected by the pumping borehole HLX10, i.e. along fracture (zone) 4. The responses may have been transmitted indirectly via local fractures.

The pressure history in the observation sections in HLX11 during the entire test period together with the precipitation during the period is shown in Figure A-25 and -26, respectively. The pressure in the observation sections in the shallow borehole HLX11 was strongly influenced by the rainfall periods. The pressure started to increase at c 17:00 hours on the 9$^{th}$ of July during the flow period due to precipitation. The maximal drawdown in sections HLX11:1 and :2 (before the rainfall) was c 2.3 and 2.4 m, respectively. The pressure recovery is also influenced by precipitation.

#### *Interpreted flow regimes*

Test diagrams in lin-log and log-log diagrams for sections HLX11:1 and :2 during the flow- and recovery period are presented in Figures A-27–30 and -31–34, respectively, in Appendix. During the flow period, a rather well-defined pseudo-radial flow regime is indicated in section HLX11:1 between c 500–4,000 min. However, it is uncertain if this regime represents the hydraulic properties of this section due to the delayed response. The recovery period seems to be dominated by leakage support from the precipitation. In section HLX11:2, a less well-defined pseudo-radial flow regime is indicated during the flow period. The pressure recovery was similar to that in section HLX11:1. No pseudo-radial flow regime occurred during recovery period, neither in section HLX11:1 nor in HLX11:2.

#### *Interpreted parameters*

An attempt to transient interpretation of the flow- and recovery period in sections HLX11:1 and HLX11:2 was made as shown in log-log and lin-log diagrams in Figures A-27-34. However, it is uncertain if the interpretations of the hydraulic properties of these sections are representative due to the delayed responses in the sections. The response analysis in Figure 5-1 indicated that the sections most likely are indirectly connected to the pumping borehole HLX10. This is also indicated by the high calculated values on the storativity for these sections. The responses during the recovery period seem to be strongly influenced by leakage support from precipitation as reflected by the apparent high value on the leakage factor r/B in the analysis. Therefore, the results of the interpretation of hydraulic parameters from the sections in HLX11 are shown within brackets in Table 5-5.

### 5.2.6 Summary of pumping test results

The results of the hydraulic evaluation of the tracer pumping test in HLX10 are summarized in Table 5-4 and 5-5. A classification of the hydraulic connections between the observation sections and the pumping borehole was made according to the Methodology study for interference tests (Index 1). Calculated hydraulic parameters from observation sections with considered bad hydraulic connection to the pumping borehole are within brackets. The hydraulic connection and geometrical interpretation of borehole HLX11 in relation to the pumping borehole HLX10 is uncertain. The evaluation of these responses is uncertain and may not be amenable for quantitative evaluation with standard methods due to the heterogeneity of the rock.

Hydraulic parameters in bold are considered most representative, selected from either the transient evaluation of the flow- or recovery period of the test. By the calculation of the skin factor for the pumping borehole, the storativity was assumed to $5.0\times10^{-5}$ which is consistent with the calculated storativity values from the observation sections. The leakage coefficient K'/b' was calculated from the value on r/B from the simulation of the tests.

Table 5-5 shows that the calculated hydraulic diffusivity for observations sections with hydraulic connection classified as "Good" is significantly higher compared to those with a "Bad" hydraulic connection. The calculated hydraulic parameters for KLX02:1 are considered as representative for the assumed fracture zone between this section and the pumping borehole HLX10. Also the hydraulic parameters for KLX02:2 may be representative for this zone and interconnecting zones. The transmissivity of these sections are in reasonable agreement with the results from the difference flow logging in KLX02 /Rouhiainen P, 2000/.

**Table 5-4. Summary of calculated hydraulic parameters from the pumping borehole during the tracer pumping test in borehole HLX10.**

| Borehole section | Section (m) | Test period | Q/s ($m^2/s$)[1] | $T_M$ ($m^2/s$)[1] | ζ (–) | $T_T$ ($m^2/s$) | S* (–) | $T_T/S^*$ ($m^2/s$) |
|---|---|---|---|---|---|---|---|---|
| HLX10 | 0–85 | Flow | $2.8\times10^{-4}$ | $3.3\times10^{-4}$ | –6 | $1.6\times10^{-4}$ | $5.0\times10^{-5}$ | 3.2 |
| " | " | Recovery | – | – | –6 | $1.4\times10^{-4}$ | $5.0\times10^{-5}$ | 2.8 |

1) Based on the maximal drawdown before the rainfall at c 17.00 hours on the 9th of July.

**Table 5-5. Summary of calculated hydraulic parameters from the observation borehole sections during the tracer pumping test in HLX10 together with a classification of the hydraulic connection between the observation sections and the pumping borehole.**

| Borehole section | Section (m) | Test period | $T_T$ ($m^2/s$) | S (–) | $T_T/S$ ($m^2/s$) | K'/b' ($s^{-1}$) | Hydraulic connection[1] |
|---|---|---|---|---|---|---|---|
| KLX02:3 | 0–206.9 | Flow | $(7.5\times10^{-5})$ | $(2.6\times10^{-4})$ | (0.3) | $(1.1\times10^{-9})$ | Bad |
| " | " | Recovery | $(8.9\times10^{-5})$ | $(1.7\times10^{-4})$ | (0.5) | $(7.1\times10^{-10})$ | " |
| KLX02:2 | 207.9–255.4 | Flow | $1.5\times10^{-4}$ | $5.0\times10^{-5}$ | 3.1 | $5.6\times10^{-11}$ | Good |
| " | " | Recovery | **$1.2\times10^{-4}$** | **$3.6\times10^{-5}$** | **3.4** | **$3.6\times10^{-11}$** | " |
| KLX02:1 | 256.4–1,700 | Flow | **$1.6\times10^{-4}$** | **$3.8\times10^{-5}$** | **4.1** | **$2.5\times10^{-11}$** | Good |
| " | " | Recovery | $1.1\times10^{-4}$ | $2.8\times10^{-5}$ | 4.0 | $3.5\times10^{-11}$ | " |
| HLX11:2 | 0–13 | Flow | $(1.2\times10^{-4})$ | $(6.8\times10^{-4})$ | (0.2) | – | Bad |
| " | " | Recovery | $(6.0\times10^{-5})$ | $(3.2\times10^{-4})$ | (0.2) | $(2.7\times10^{-9})$ | " |
| HLX11:1 | 14–31 | Flow | $(1.6\times10^{-4})$ | $(3.9\times10^{-4})$ | (0.4) | – | Bad |
| " | " | Recovery | $(7.8\times10^{-5})$ | $(2.8\times10^{-4})$ | (0.3) | $(4.8\times10^{-9})$ | " |

[1] According to the classification of responses (Index 1) in the methodology description for Interference tests.

Q/s = specific flow,
$T_M$ = steady-state transmissivity from Moye´s formula,
$T_T$ = calculated transmissivity from transient evaluation of the test,
$S^*$ = assumed value on storativity,
S = calculated value on storativity from transient evaluation of the test,
$T_T/S$ = calculated hydraulic diffusivity from transient evaluation of the test,
K'/b' = calculated leakage coefficient from transient evaluation of the test,
ζ = calculated skin factor from transient evaluation of the test.

# 6 Discussion and conclusions

The combined pumping and tracer test did not give any tracer breakthrough for the 260 m flow path between KLX02:2 and HLX10. The most plausible explanation for this is that the flow geometry probably is more complicated than assumed. The analysis shows indirect responses in KLX02:2 indicating that more than one fracture/fracture zone are involved in the transport. The analysis shows a possible interpretation that the tracer injected in KLX02:2 first is transported through a set of steep fractures down to the conductive fracture 4 intersecting KLX02 at 317 m, and then towards HLX10. This flow path is considerably longer than 260 m and the two week pumping period was possibly too short.

The hydraulic parameters calculated from KLX02:1 pressure responses are considered as representative for fracture 4 and the transmissivity is in reasonable agreement with the results from the difference flow logging in KLX02.

Pumping in HLX10 only generated weak and uncertain pressure responses in observation well HLX11. Although both boreholes intersect the gently dipping fracture/fracture zone "A", determined from seismic survey, the weak and uncertain pressure responses indicates zone "A" is a poor hydraulic conductor at this location.

# 7 References

**Ekman L (ed), 2001.** Project Deep Drilling KLX02 – Phase 2. Methods, scope of activities and results. Summary report. SKB TR-01-11. Svensk Kärnbränslehantering AB.

**Carlsten S, Stråhle A, Ludvigson J-E, 2001.** Conductive fracture mapping. A study on the correlation between borehole TV- and radar images and difference flow logging results in borehole KLX02. SKB R-01-48. Svensk Kärnbränslehantering AB.

**Rouhiainen P, 2000.** Difference flow measurements in borehole KLX02 at Laxemar. Äspö Hard Rock Laboratory. SKB IPR-01-06. Svensk Kärnbränslehantering AB.

# Appendix

## Test data diagrams and interpretations

**Nomenclature used in diagrams from Aqtesolv:**

T = transmissivity ($m^2/s$),

S = storativity (–),

$K_Z/K_r$ = ratio of hydraulic conductivities in the vertical and radial direction (set to 1),

$S_w$ = skin factor,

r(w) = borehole radius (m),

r(c) = effective casing radius (m),

r/B = leakage factor,

C = well loss constant (set to 0).

**Diagrams**

- Flow rate, precipitation and atmospheric pressure (lin-lin).
- Pressure history during the entire test period (lin-lin).
- Flow period (log-log and lin-log).
- Recovery period (log-log and lin-log).

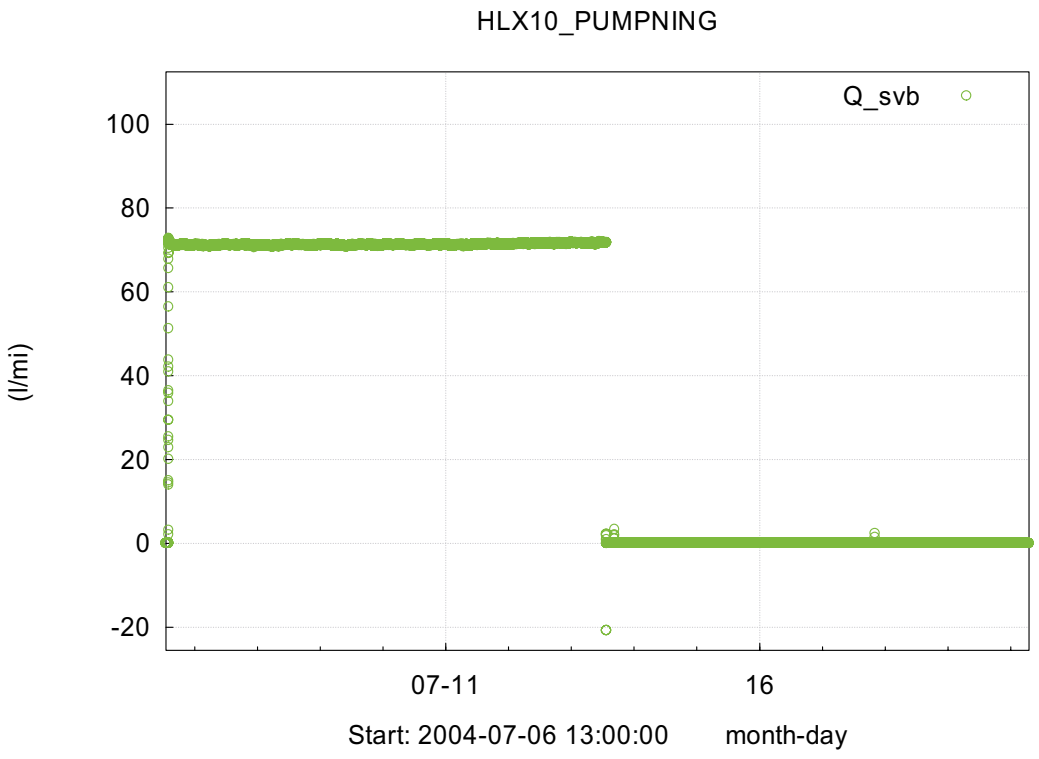


***Figure A-1.*** *Linear plot of flow rate from the pumping borehole HLX10 during the tracer pumping test.*

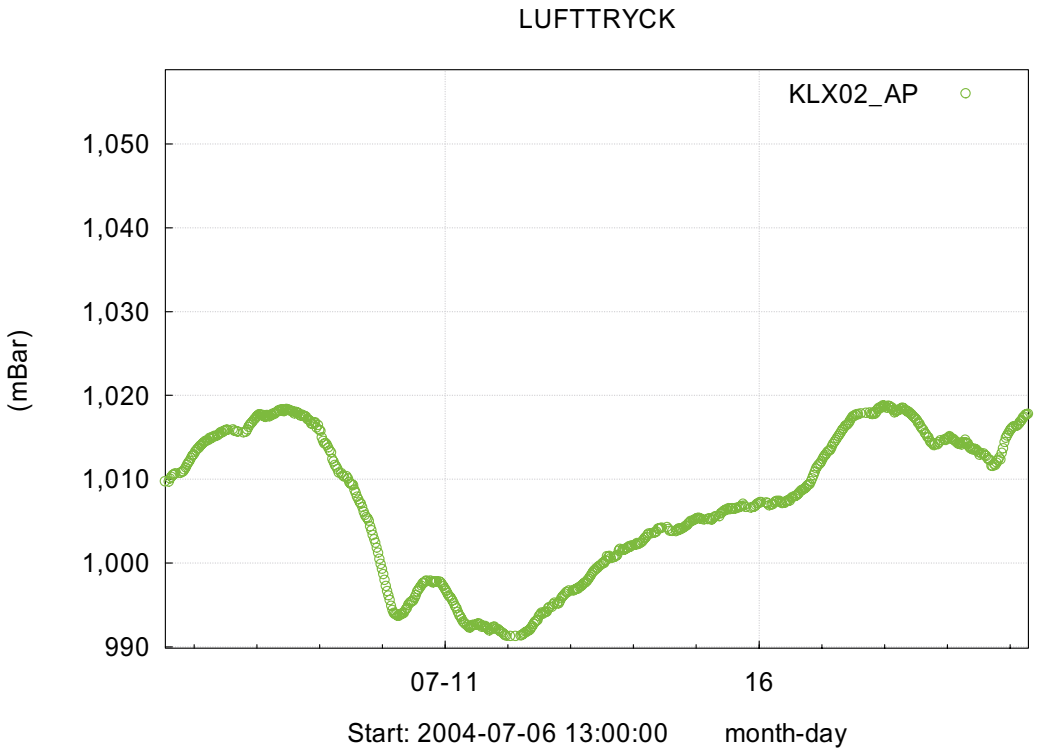


***Figure A-2.*** *Linear plot of atmospheric pressure during the tracer pumping test in HLX10.*

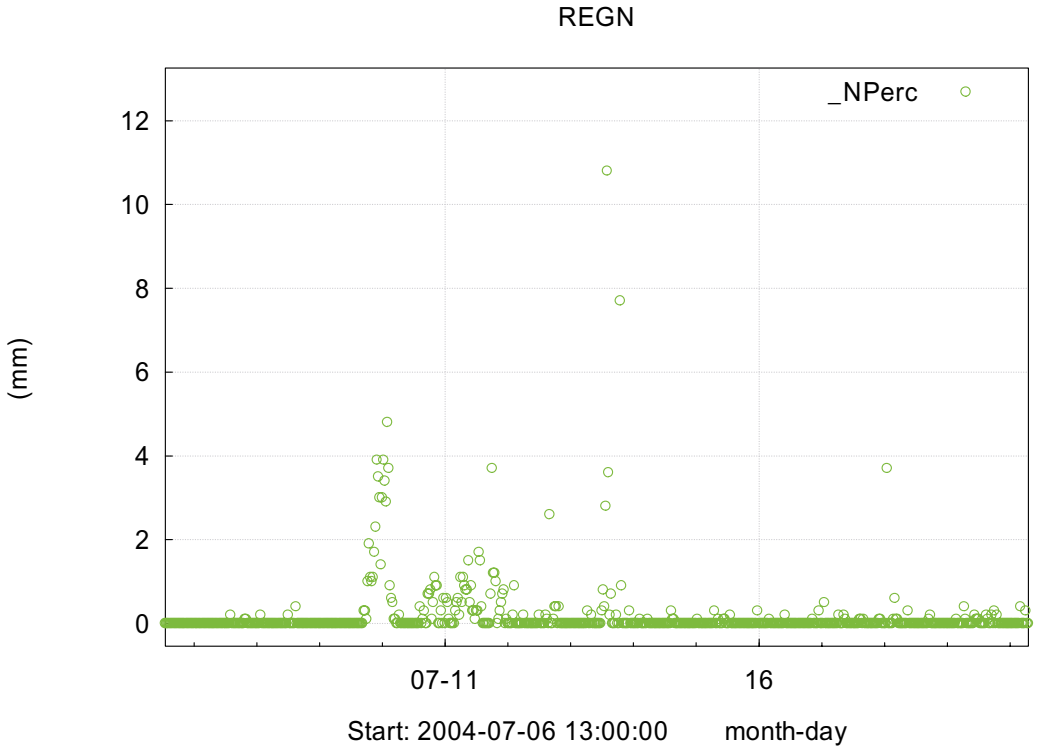

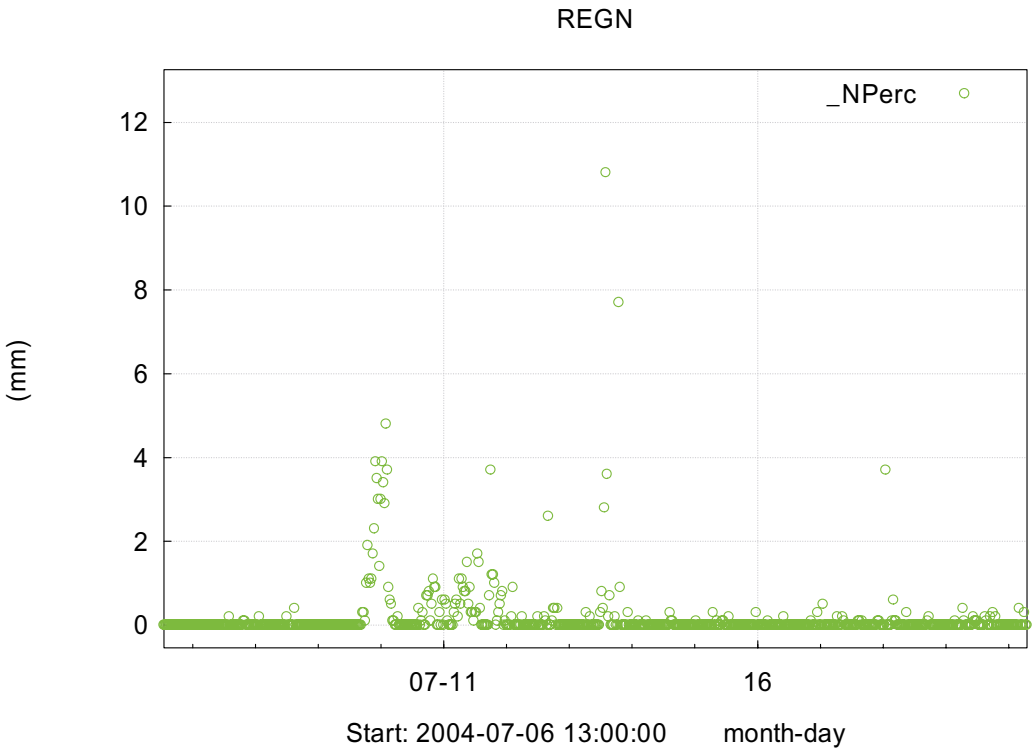


***Figure A-3.*** *Linear plot of precipitation during the tracer pumping test in HLX10.*

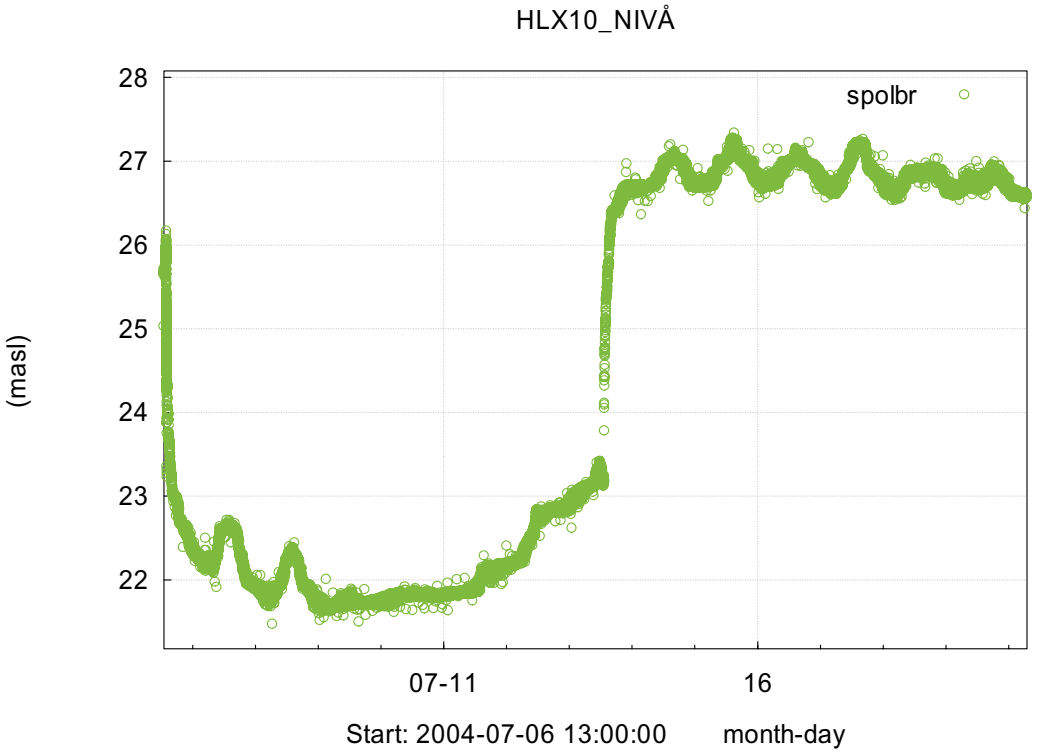


***Figure A-4.*** *Linear plot of the pressure history during the tracer pumping test in HLX10.*

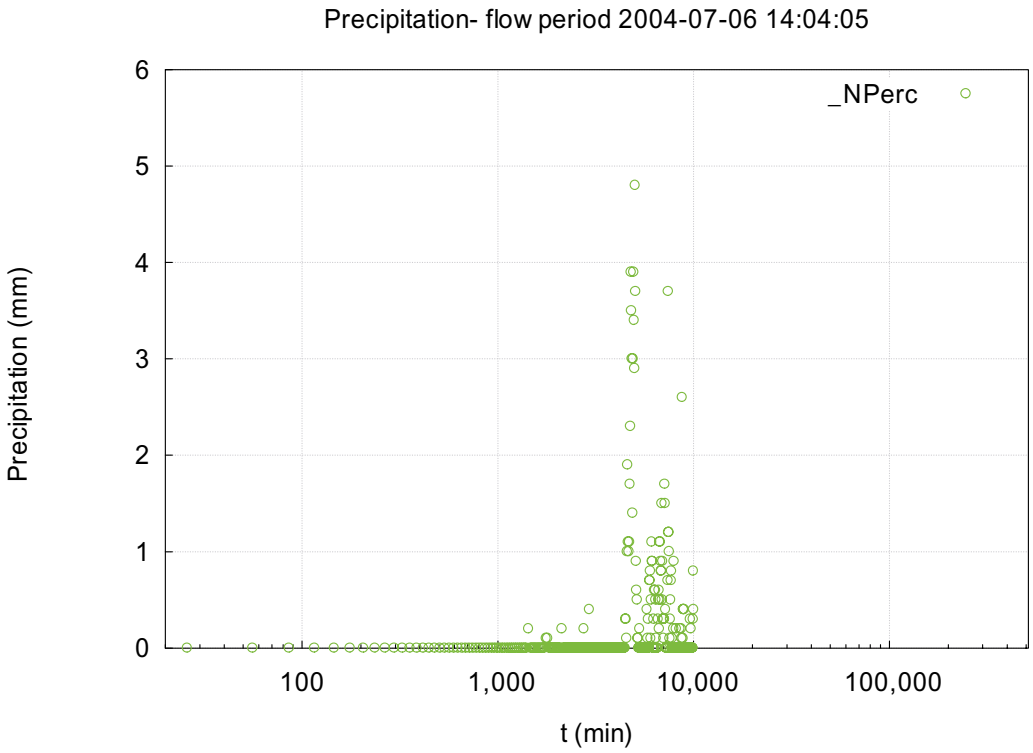


***Figure A-5.*** *Lin-Log plot of precipitation during the flow period of the tracer pumping test in HLX10.*

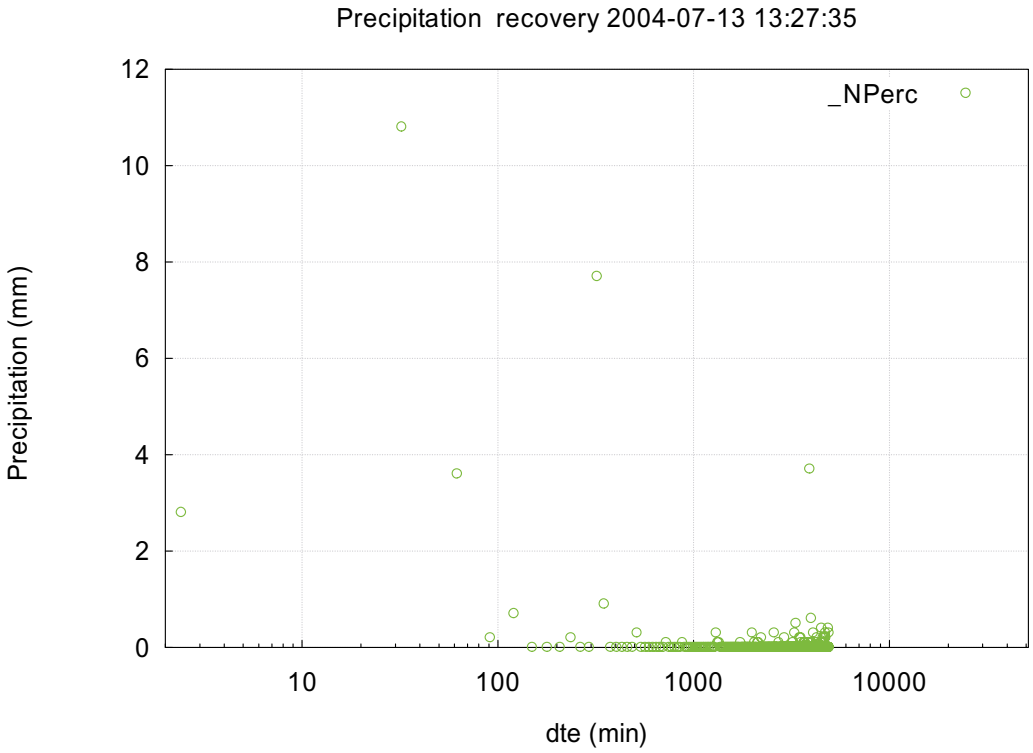


***Figure A-6.*** *Lin-Log plot of precipitation during the recovery period of the tracer pumping test in HLX10.*

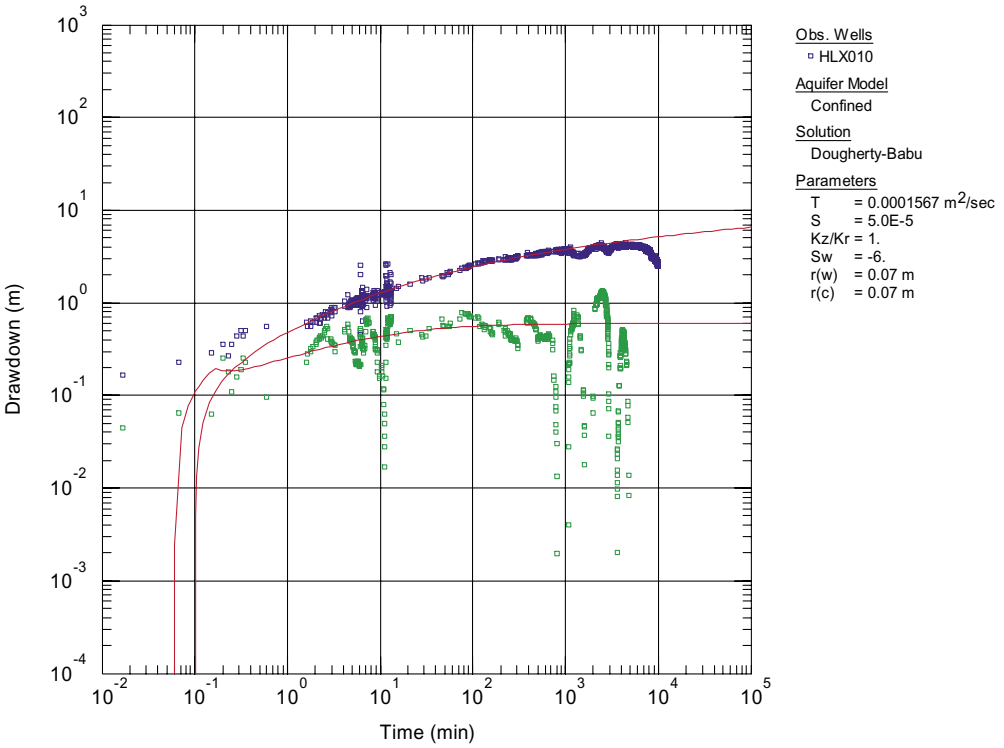


***Figure A-7.*** *Log-log plot of measured (blue) and simulated (red) pressure drawdown and – derivative (green) versus time during the flow period in the pumping borehole HLX10.*

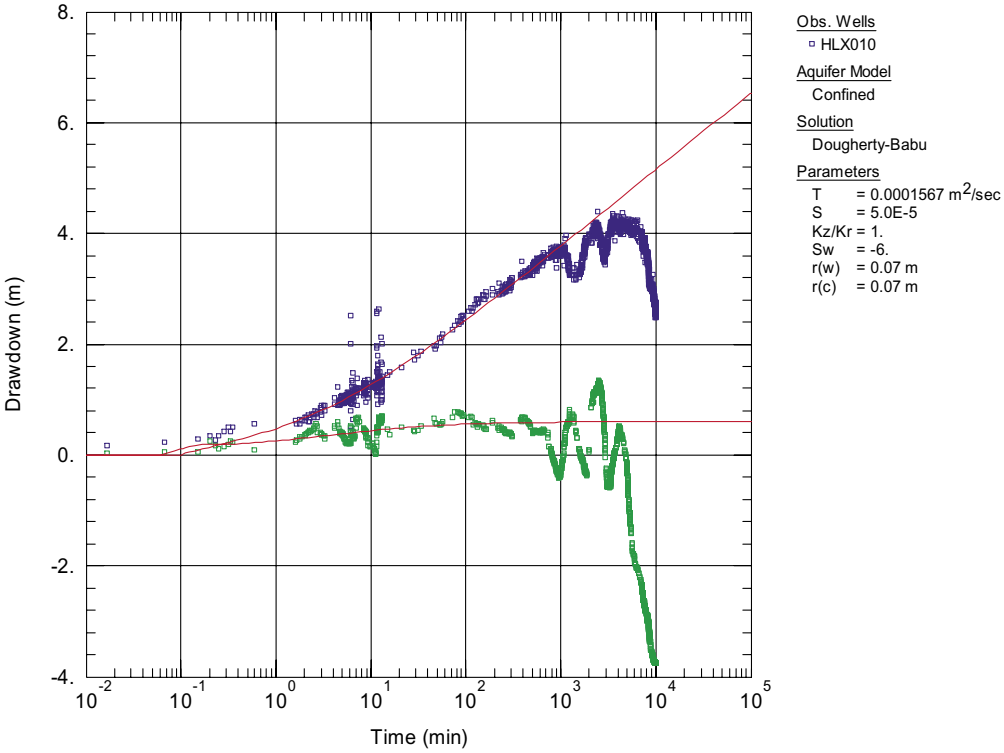


***Figure A-8.*** *Lin-log plot of measured (blue) and simulated (red) pressure drawdown and – derivative (green) versus time during the flow period in the pumping borehole HLX10.*

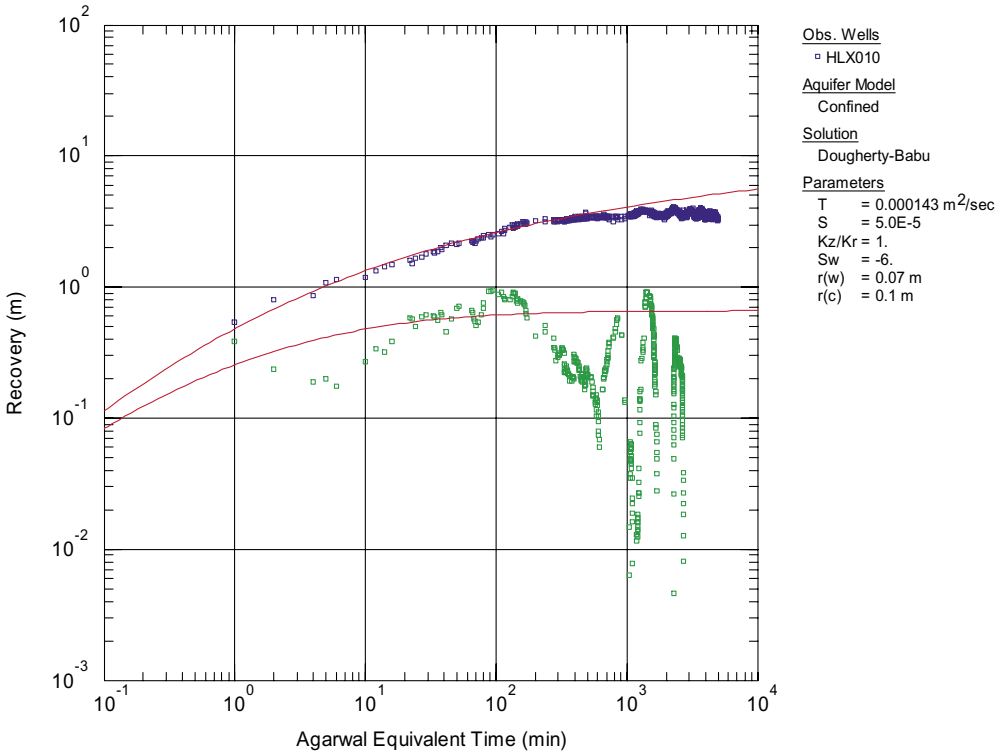


***Figure A-9.*** *Log-log plot of measured (blue) and simulated (red) pressure recovery and – derivative (green) versus equivalent time during the recovery period in borehole HLX10.*

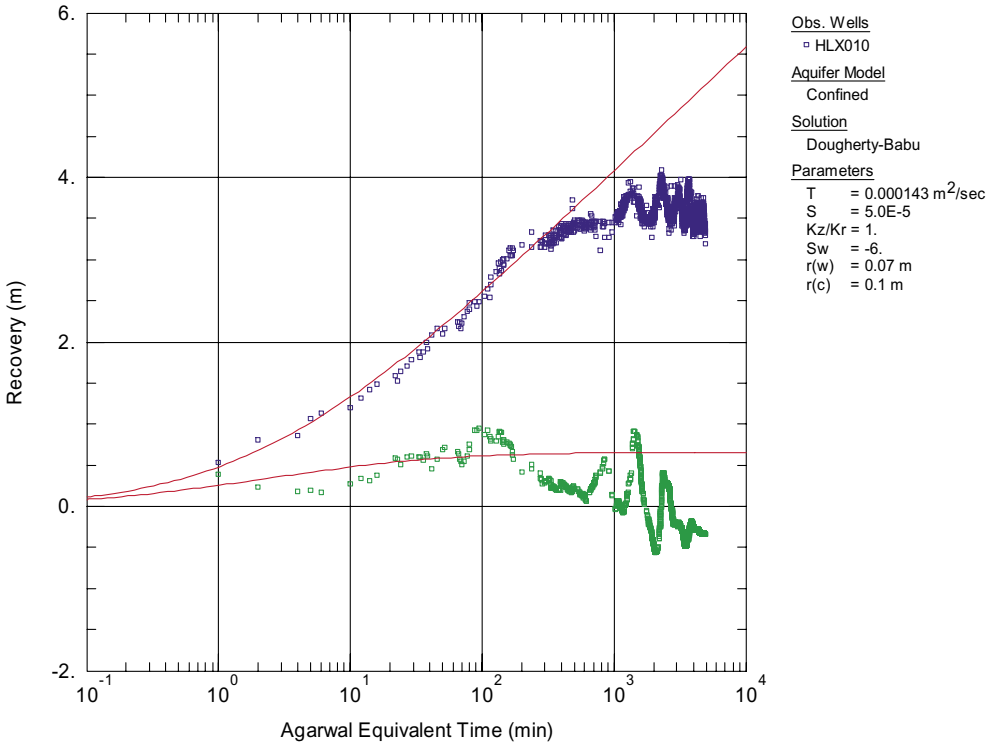


***Figure A-10.*** *Lin-log plot of measured (blue) and simulated (red) pressure recovery and – derivative (green) versus equivalent time during the recovery period in borehole HLX10.*

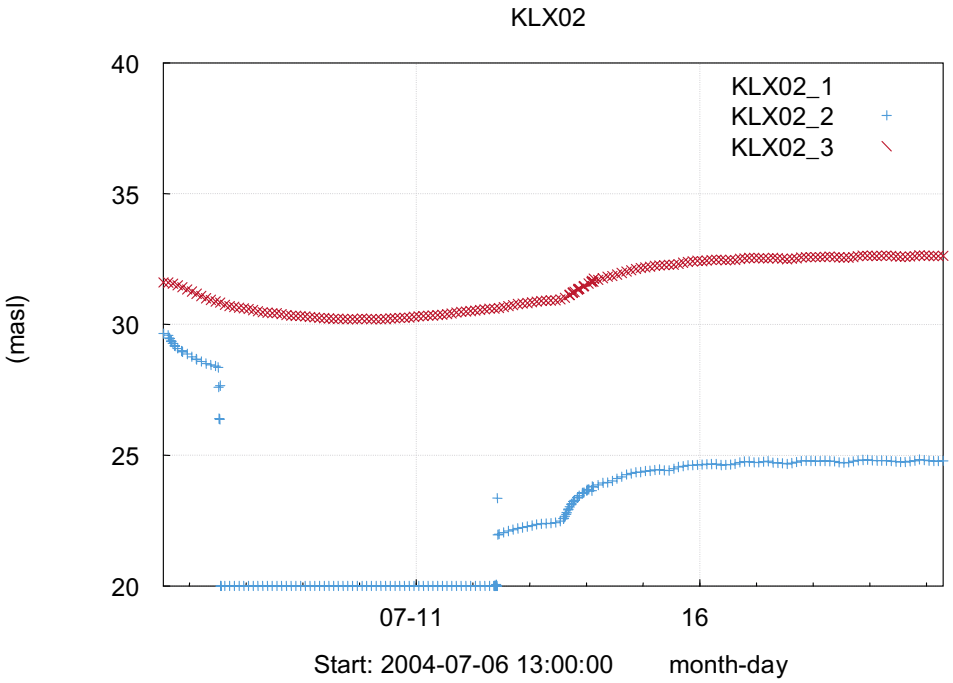


***Figure A-11.*** *Linear plot of the pressure history in observation borehole KLX02 during the tracer pumping test in HLX10. The pressure transducer in section KLX02:2 were removed during tracer injection and re-installed at a shallower depth below ground surface, see Chapter 5.2.3.*

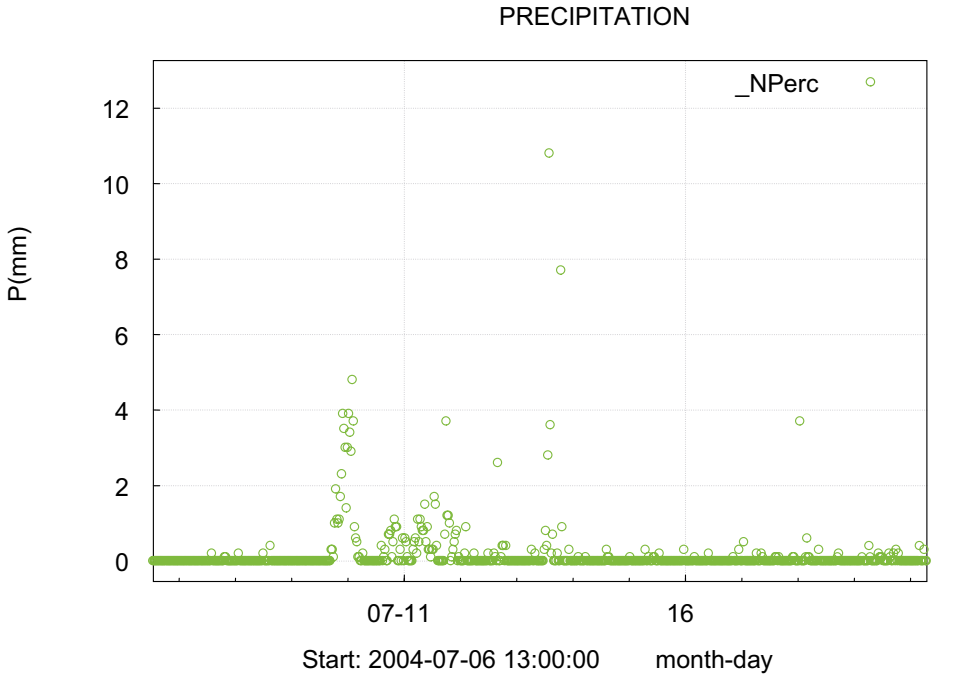


***Figure A-12.*** *Linear plot of precipitation during the tracer pumping test in HLX10.*

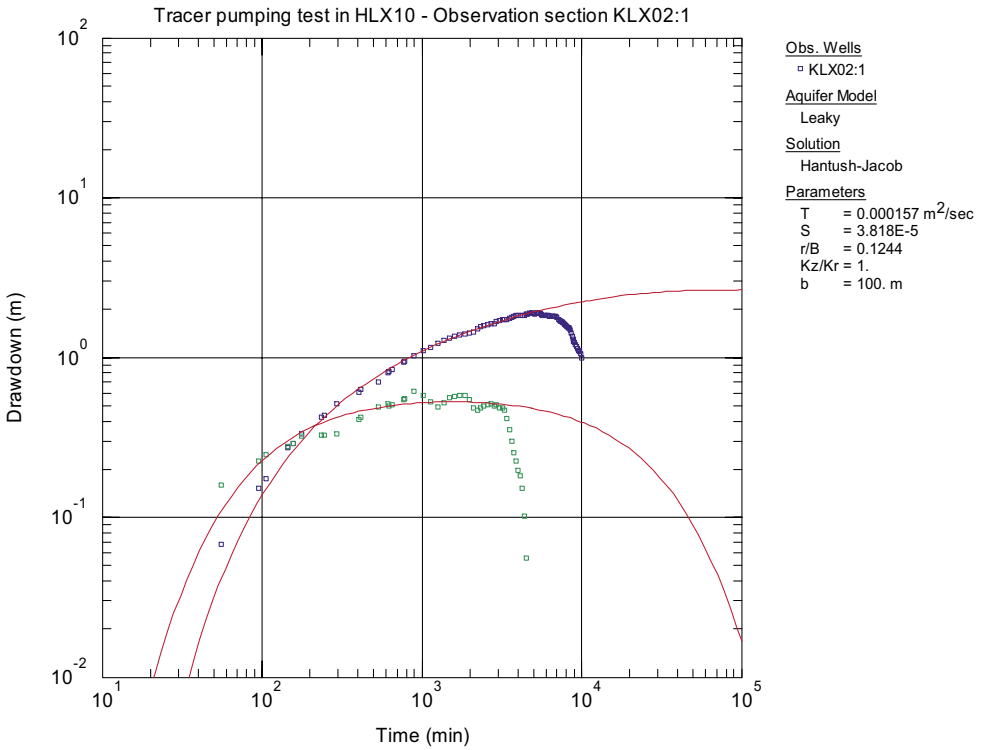


***Figure A-13.*** *Log-log plot of measured (blue) and simulated (red) pressure drawdown and – derivative (green) versus time during the flow period in section KLX02:1.*

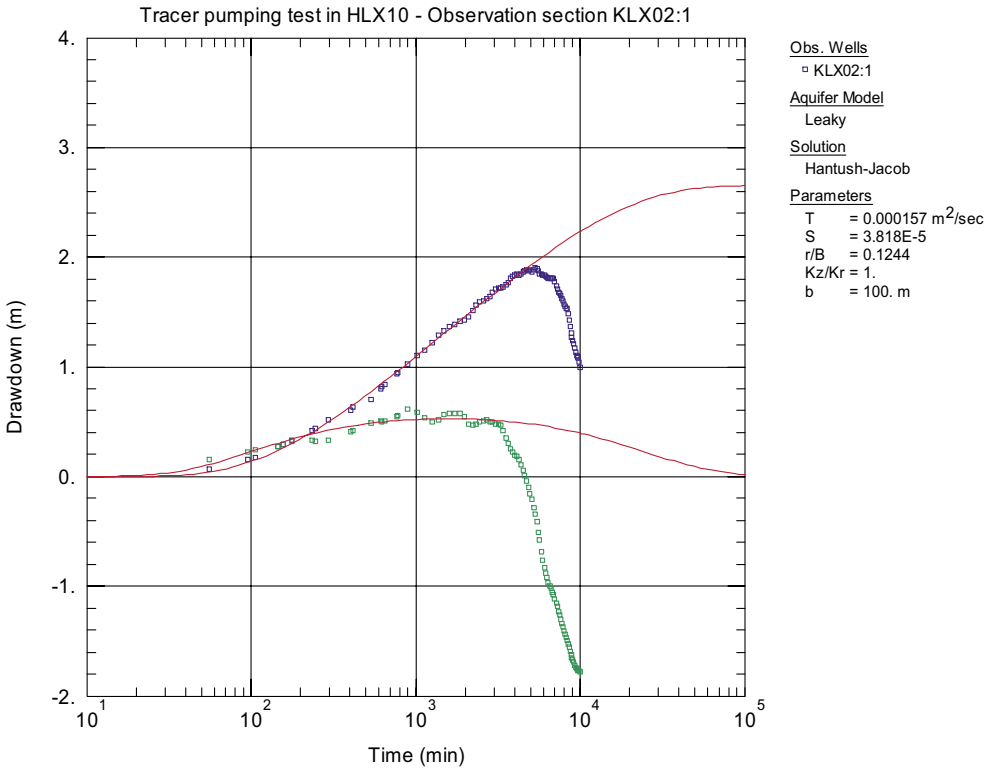


***Figure A-14.*** *Lin-log plot of measured (blue) and simulated (red) pressure drawdown and – derivative (green) versus time during the flow period in section KLX02:1.*

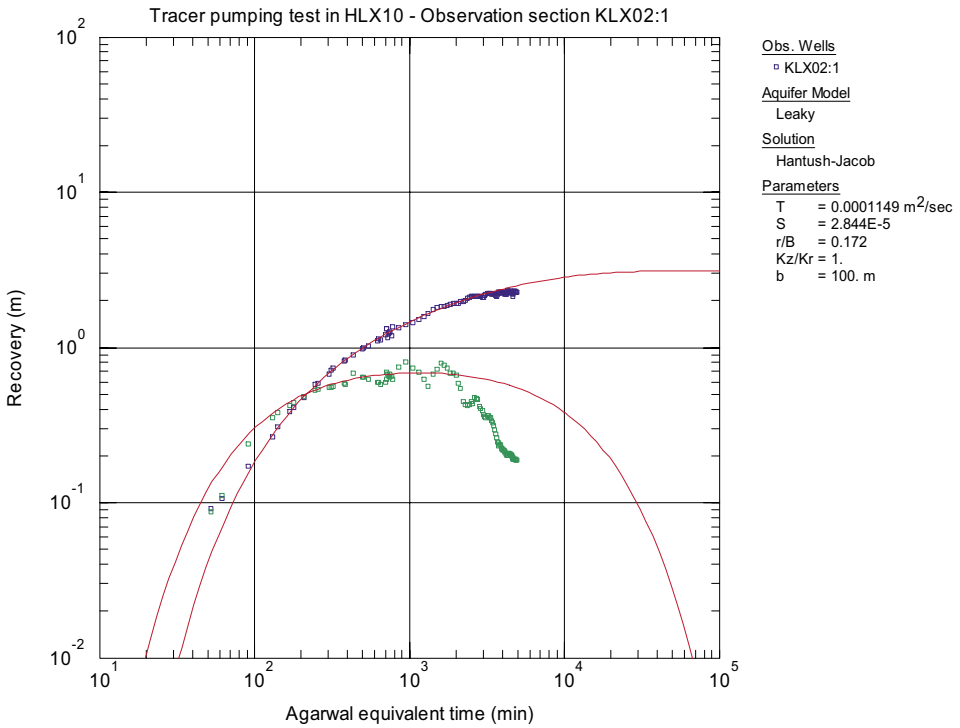


***Figure A-15.*** *Log-log plot of measured (blue) and simulated (red) pressure recovery and – derivative (green) versus equivalent time during the recovery period in section KLX02:1.*

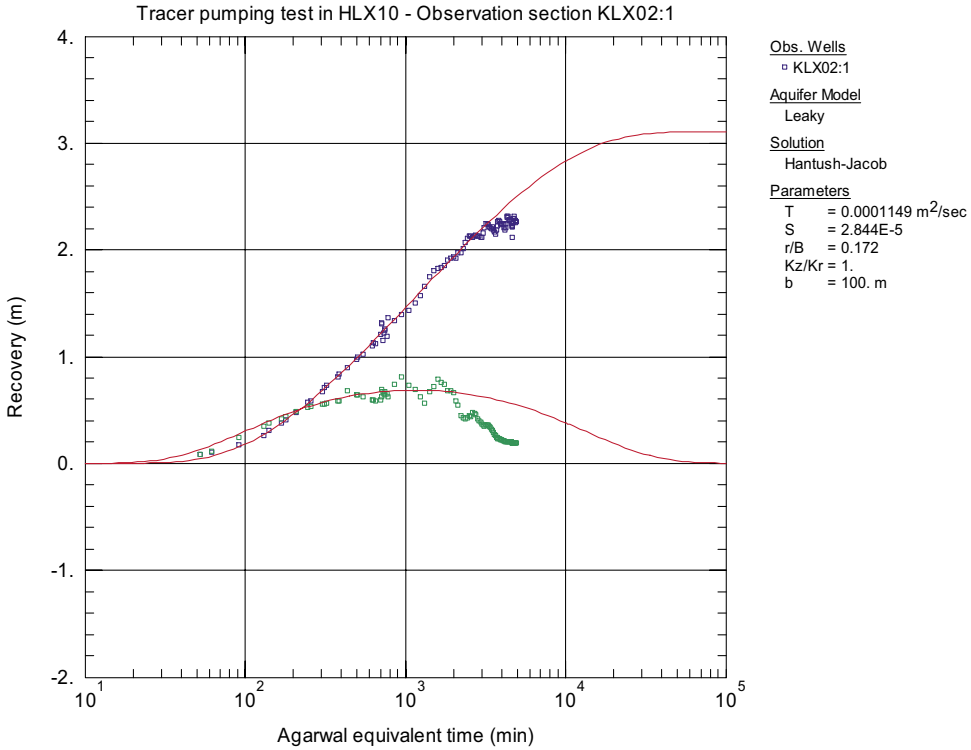


***Figure A-16.*** *Lin-log plot of measured (blue) and simulated (red) pressure recovery and – derivative (green) versus equivalent time during the recovery period in section KLX02:1.*

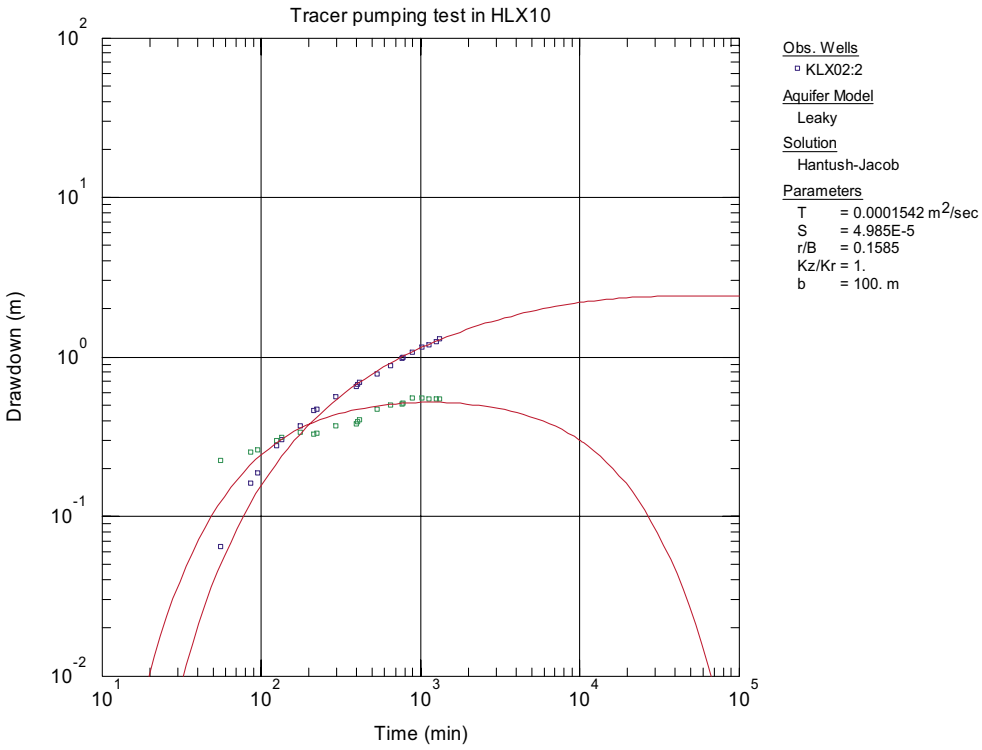


***Figure A-17.*** *Log-log plot of measured (blue) and simulated (red) pressure drawdown and – derivative (green) versus time during the flow period in section KLX02:2.*

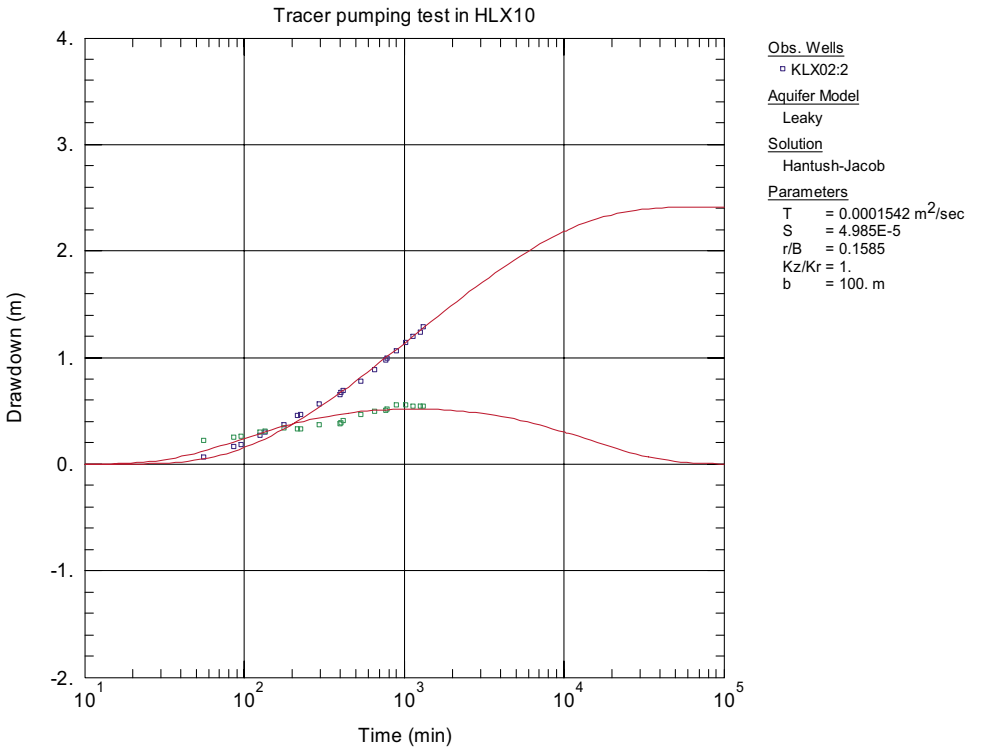


***Figure A-18.*** *Lin-log plot of measured (blue) and simulated (red) pressure drawdown and – derivative (green) versus time during the flow period in section KLX02:2.*

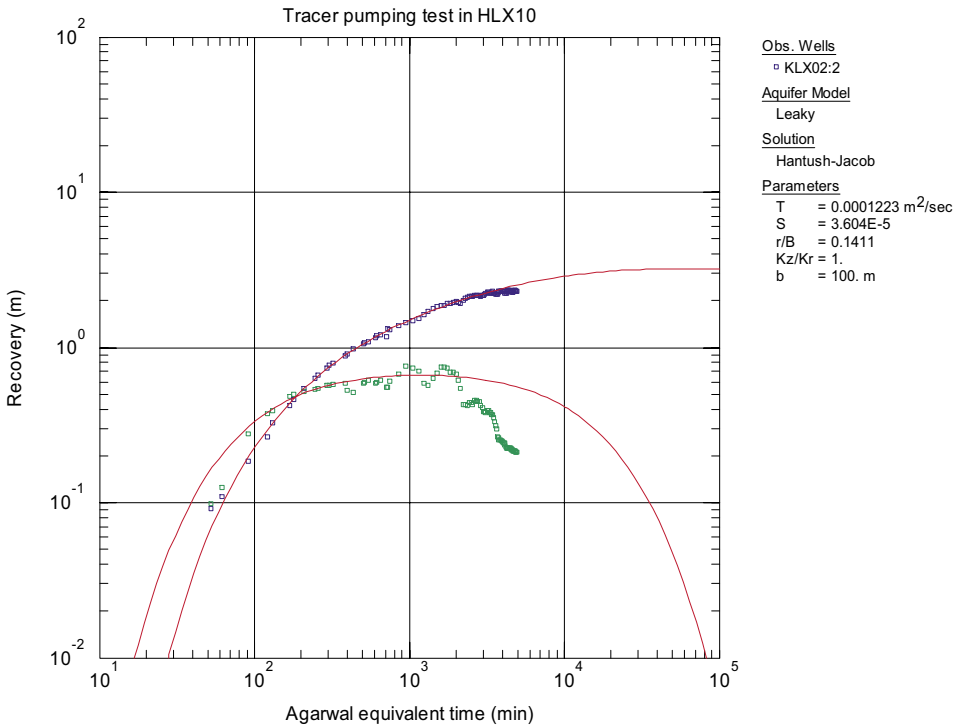


***Figure A-19.*** *Log-log plot of measured (blue) and simulated (red) pressure recovery and – derivative (green) versus equivalent time during the recovery period in section KLX02:2.*

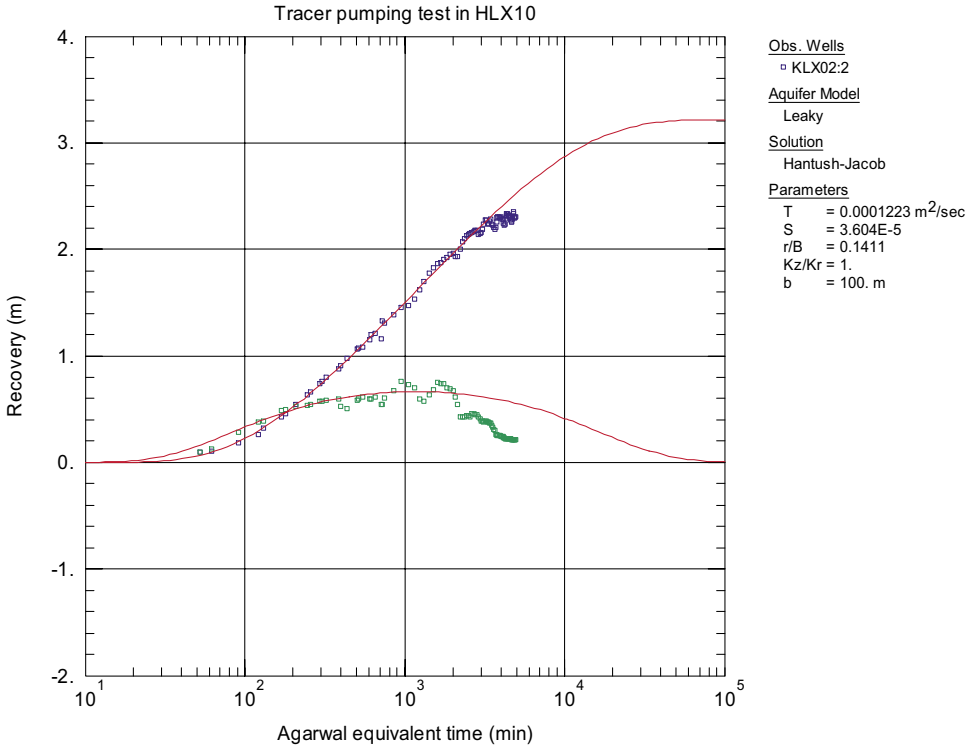


***Figure A-20.*** *Lin-log plot of measured (blue) and simulated (red) pressure recovery and – derivative (green) versus equivalent time during the recovery period in section KLX02:2.*

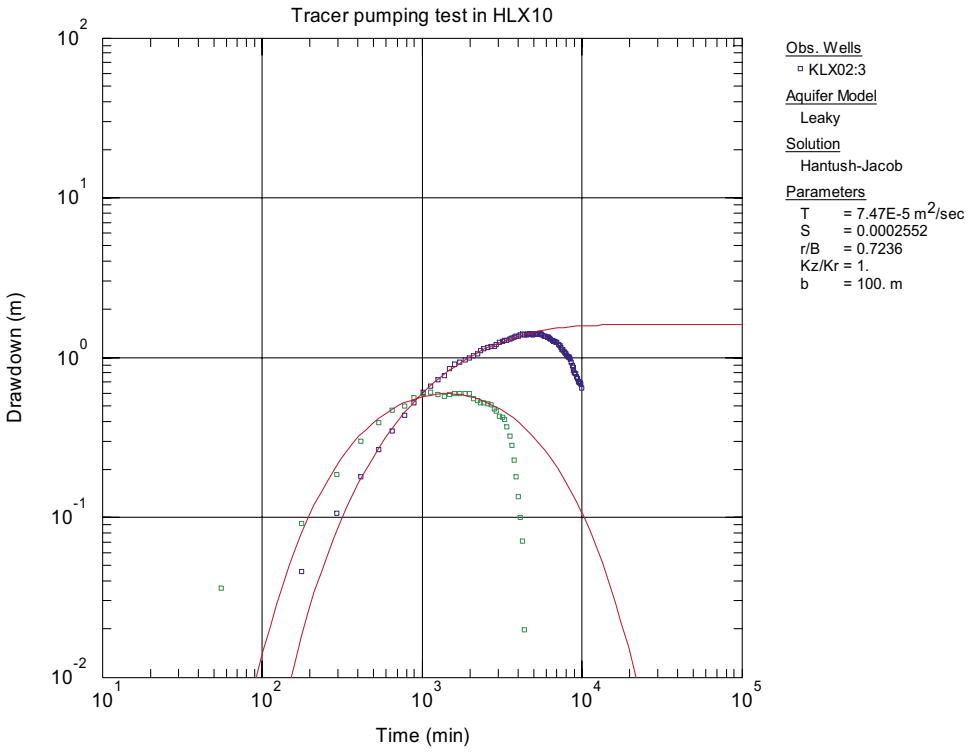


***Figure A-21.*** *Log-log plot of measured (blue) and simulated (red) pressure drawdown and – derivative (green) versus time during the flow period in section KLX02:3.*

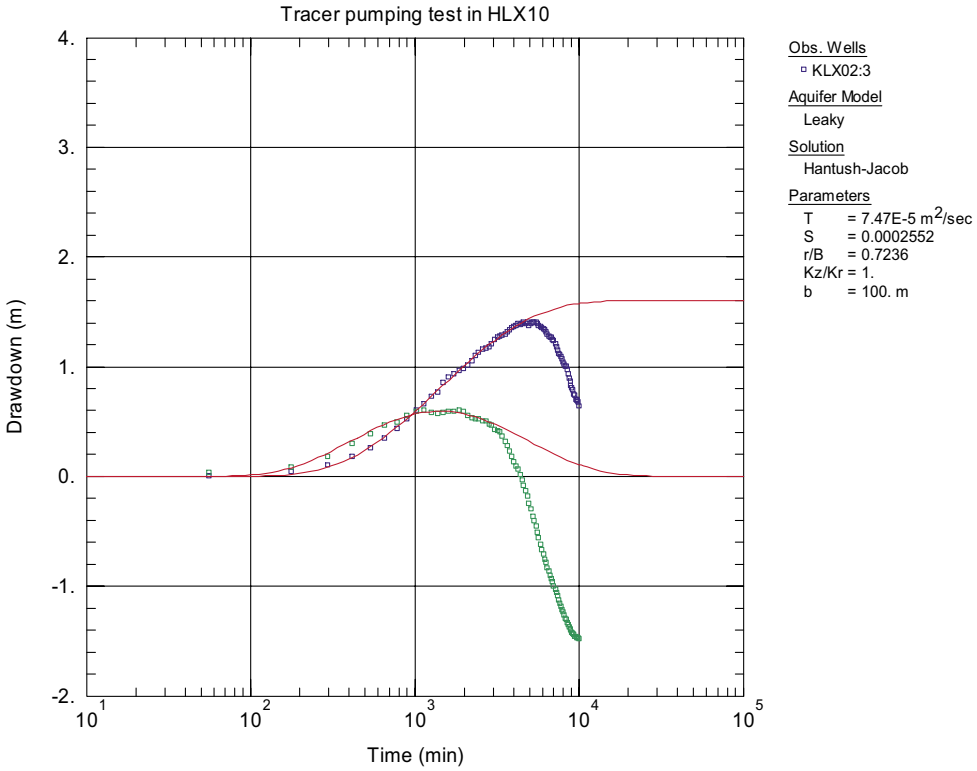


***Figure A-22.*** *Lin-log plot of measured (blue) and simulated (red) pressure drawdown and – derivative (green) versus time during the flow period in section KLX02:3.*

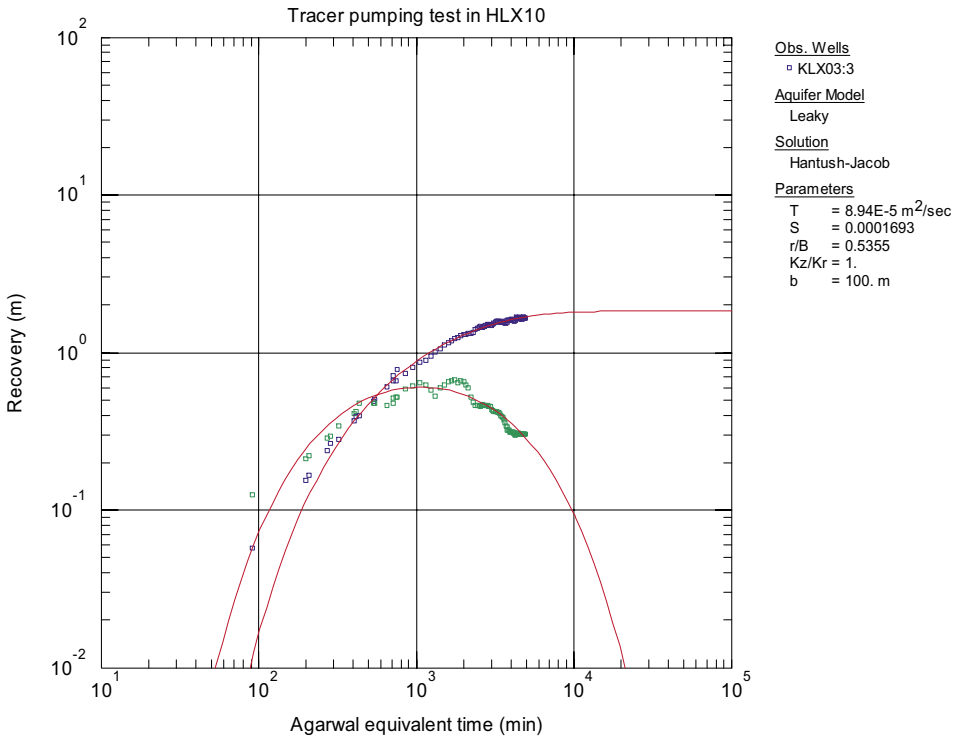


***Figure A-23.*** *Log-log plot of measured (blue) and simulated (red) pressure recovery and – derivative (green) versus equivalent time during the recovery period in section KLX02:3.*

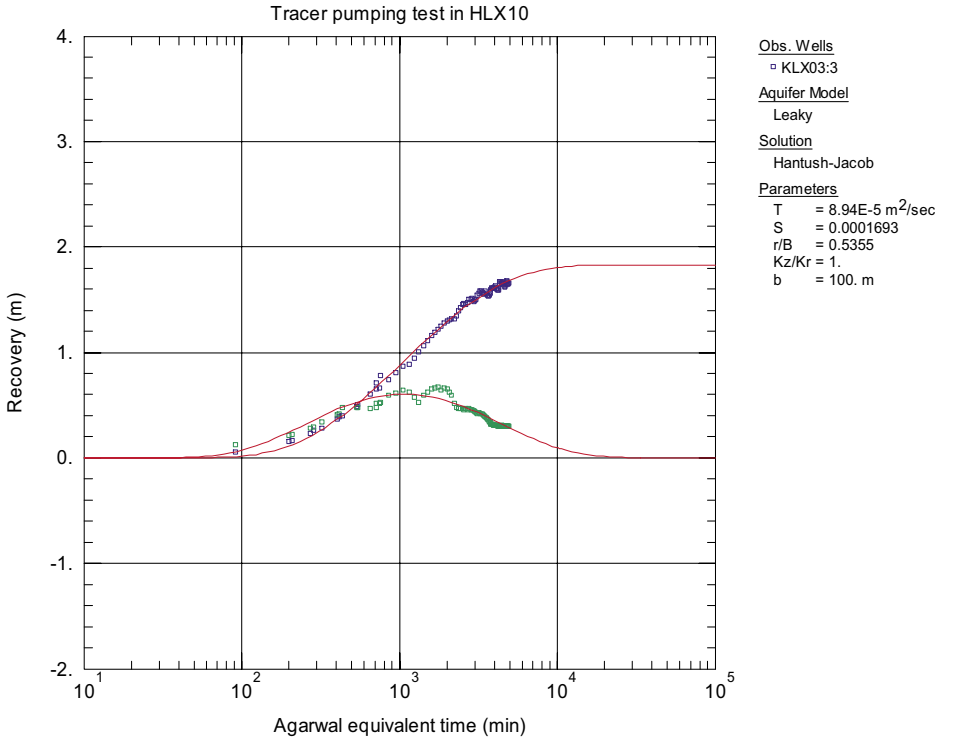


***Figure A-24.*** *Lin-log plot of measured (blue) and simulated (red) pressure recovery and – derivative (green) versus equivalent time during the recovery period in section KLX02:3.*

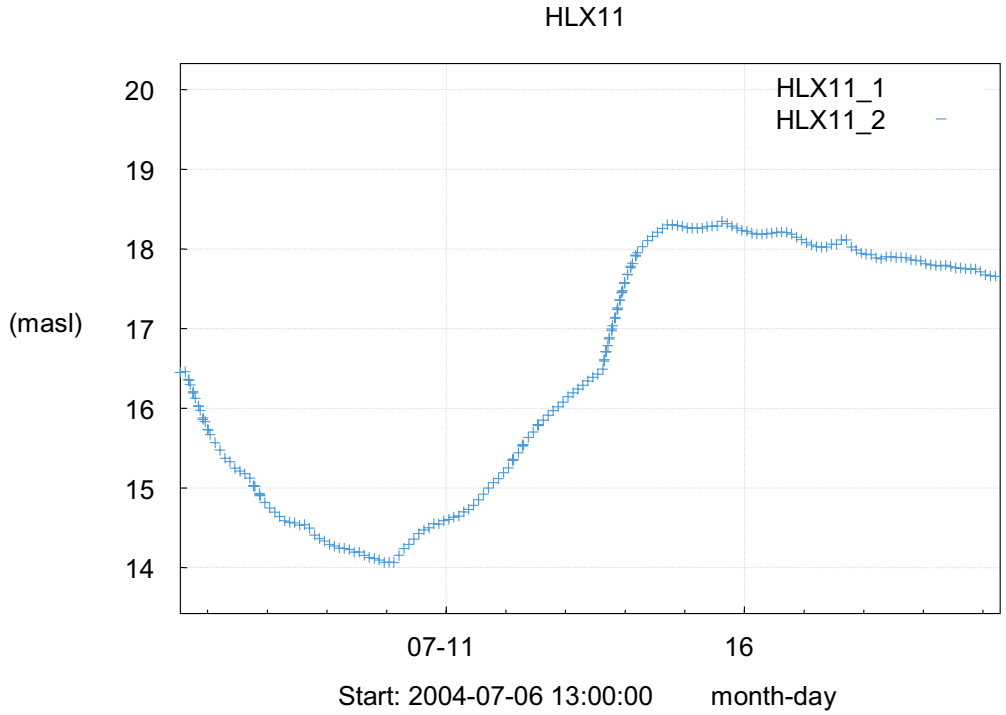


***Figure A-25.*** *Linear plot of the pressure history in observation borehole HLX11 during the tracer pumping test in HLX10.*

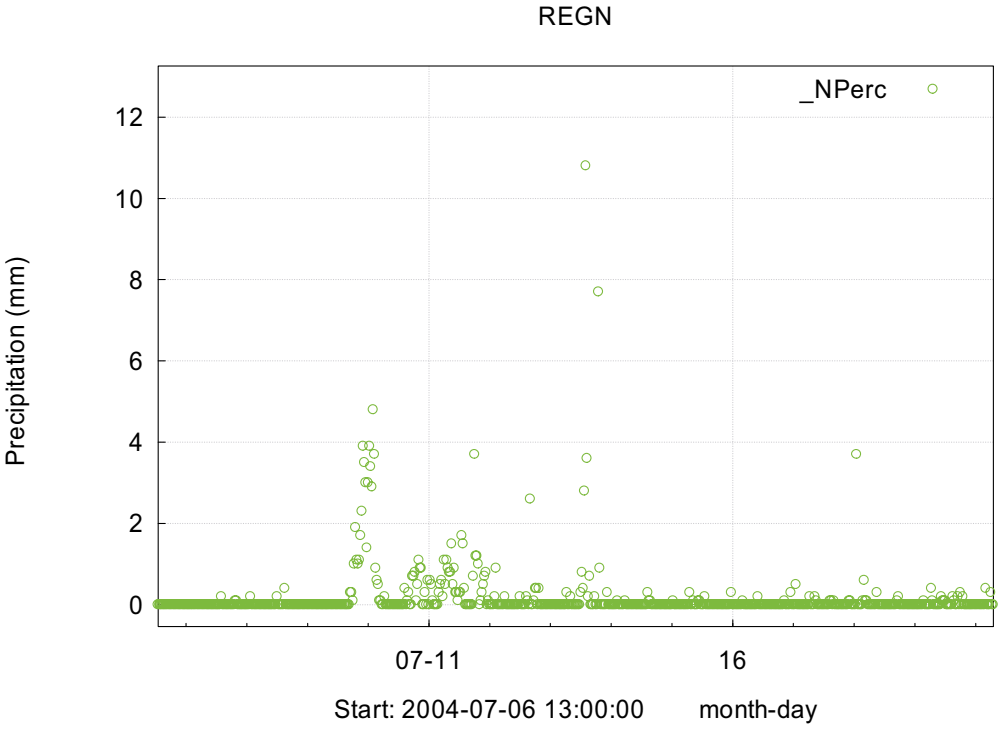


***Figure A-26.*** *Linear plot of precipitation during the tracer pumping test in HLX10.*

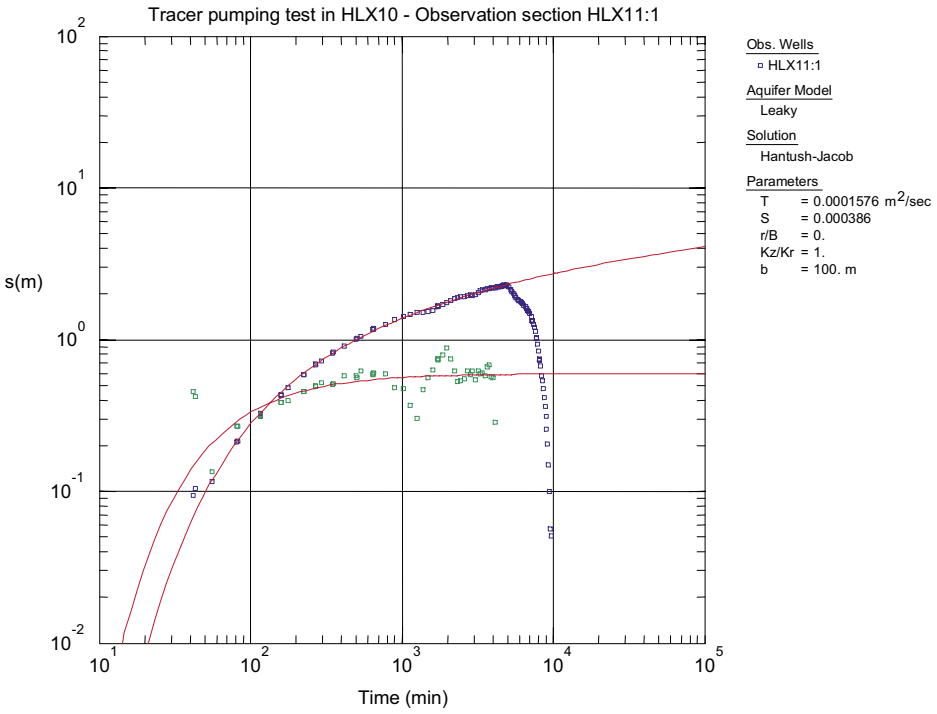


***Figure A-27.*** *Log-log plot of measured (blue) and simulated (red) pressure drawdown and – derivative (green) versus time during the flow period in section HLX11:1.*

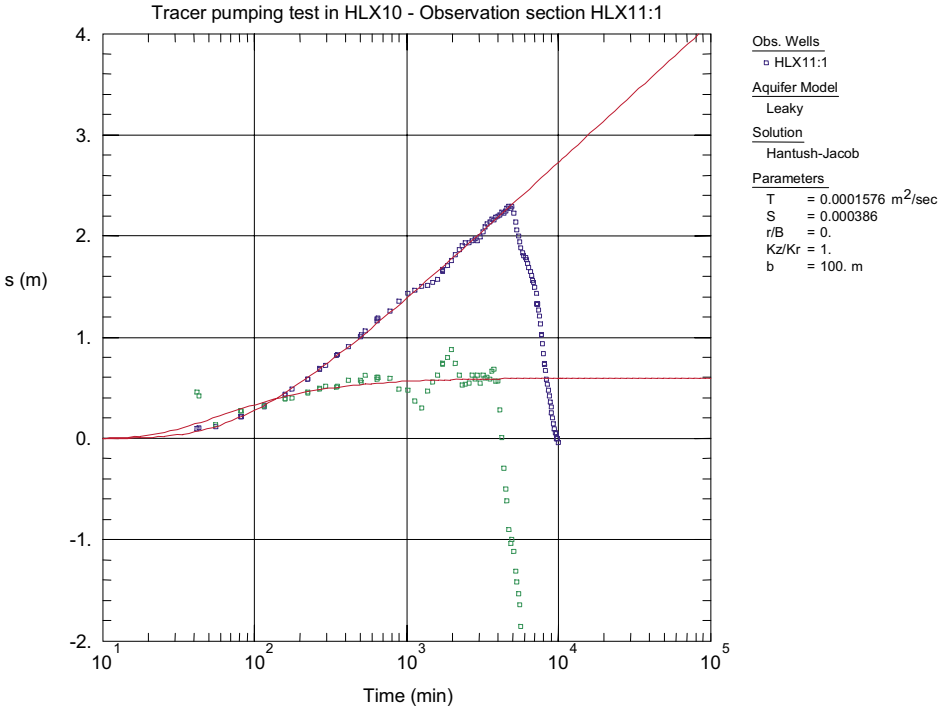


***Figure A-28.*** *Lin-log plot of measured (blue) and simulated (red) pressure drawdown and – derivative (green) versus time during the flow period in section HLX11:1.*

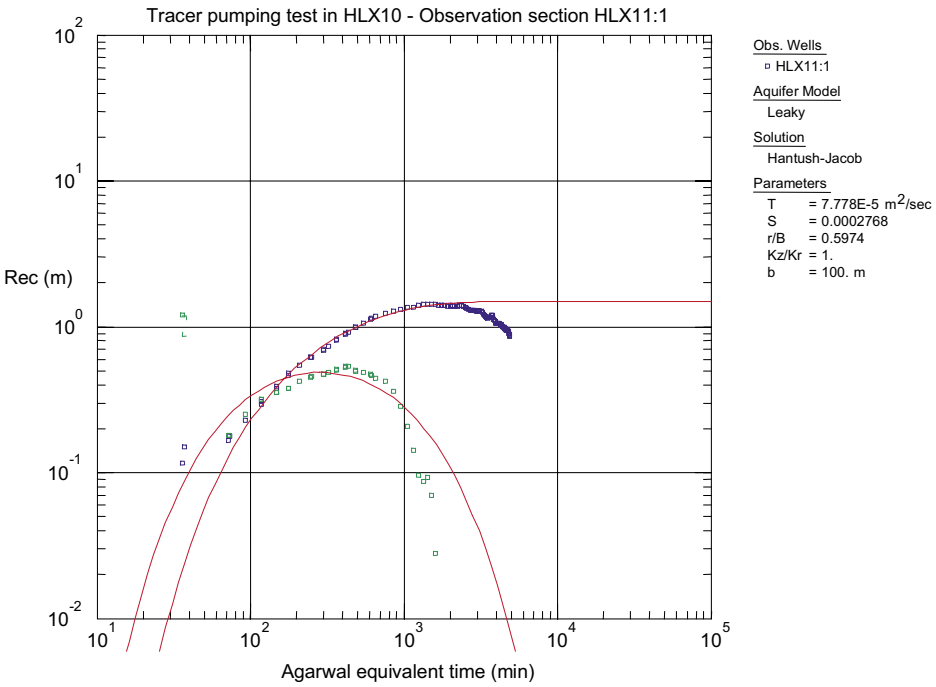


***Figure A-29.*** *Log-log plot of measured (blue) and simulated (red) pressure recovery and – derivative (green) versus equivalent time during the recovery period in HLX11:1.*

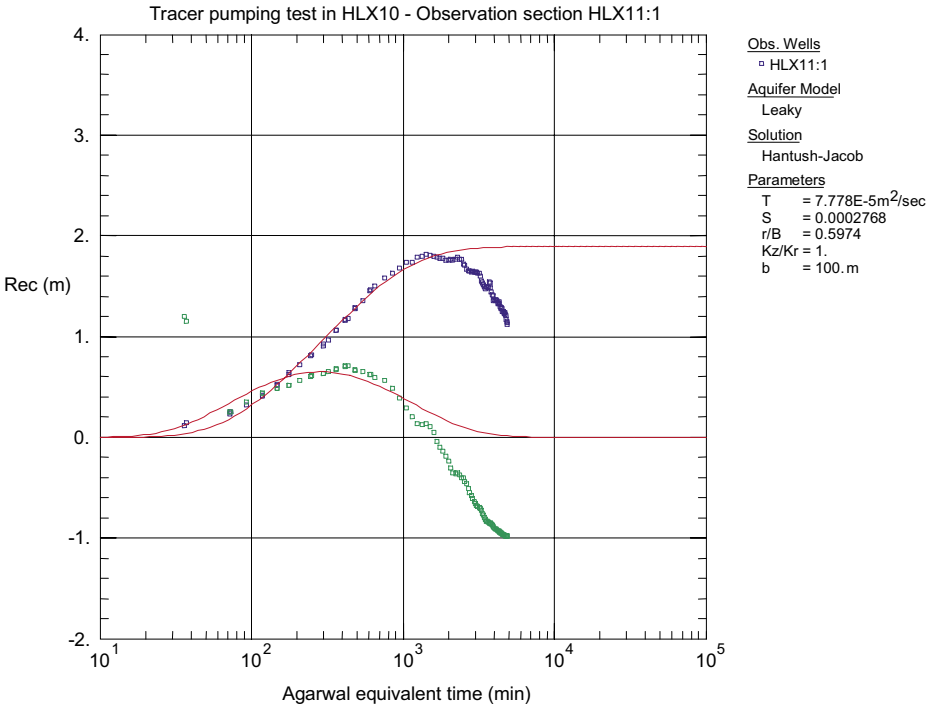


***Figure A-30.*** *Lin-log plot of measured (blue) and simulated (red) pressure recovery and – derivative (green) versus equivalent time during the recovery period in HLX11:1.*

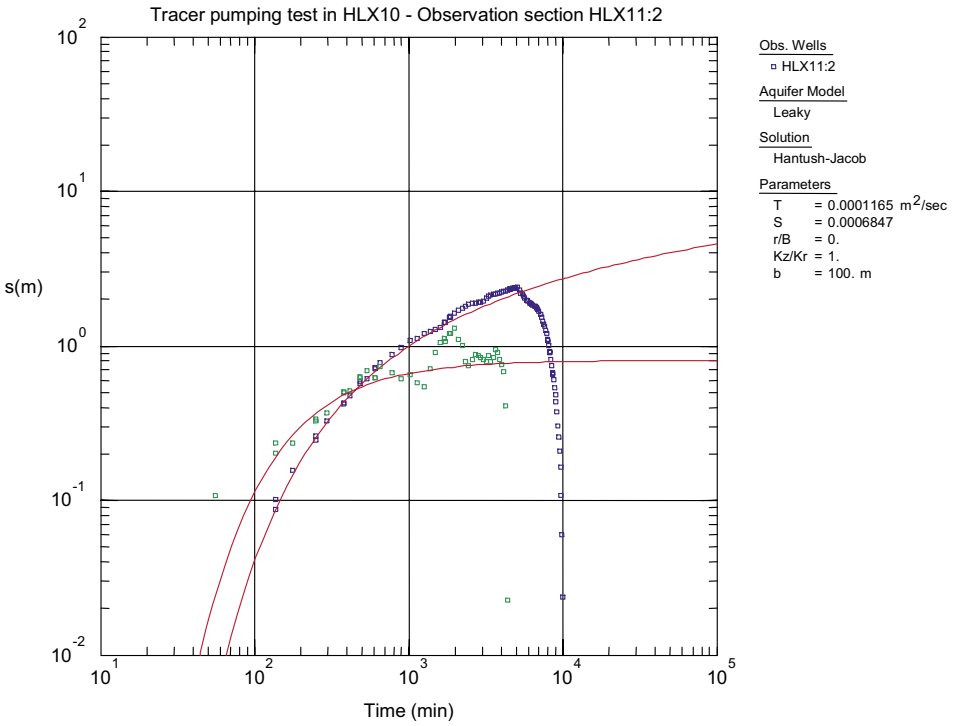


***Figure A-31.*** *Log-log plot of measured (blue) and simulated (red) pressure drawdown and – derivative (green) versus time during the flow period in section HLX11:2.*

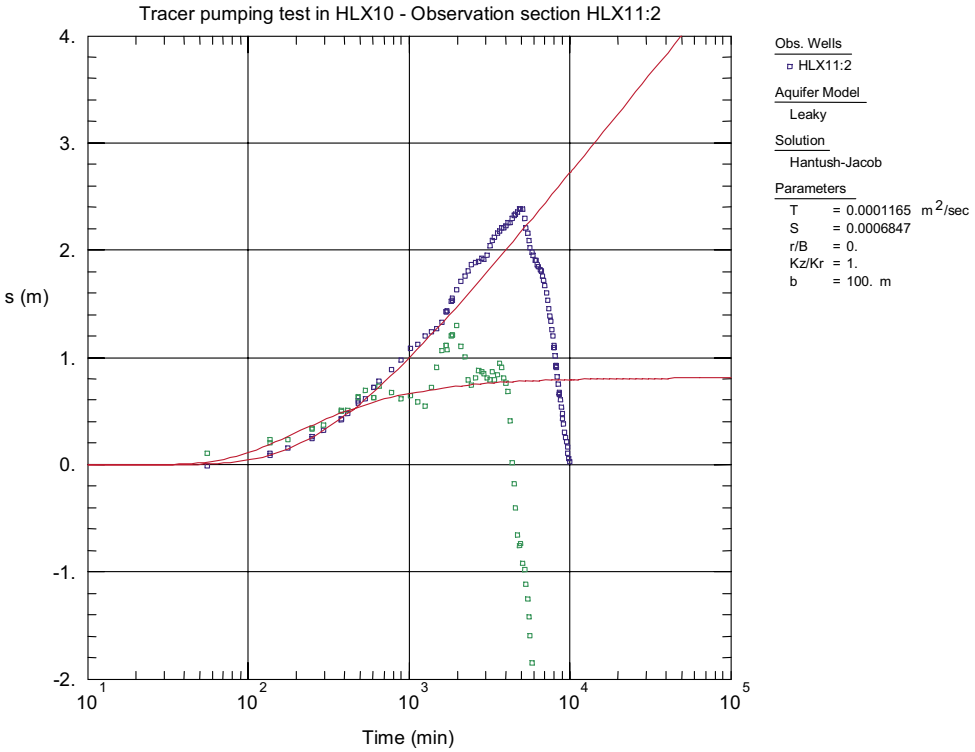


***Figure A-32.*** *Lin-log plot of measured (blue) and simulated (red) pressure drawdown and – derivative (green) versus time during the flow period in section HLX11:2.*

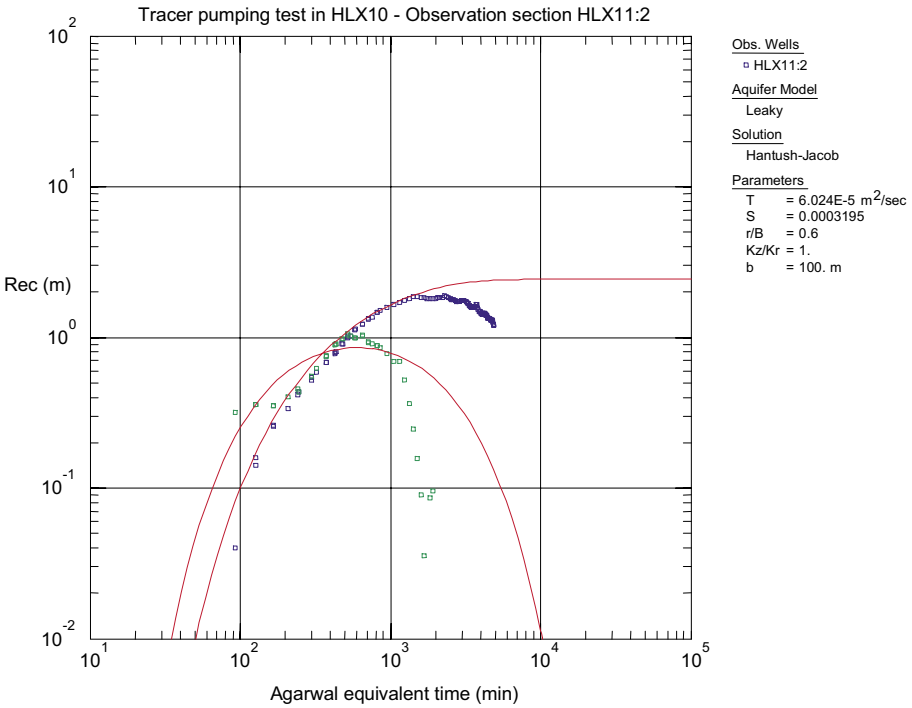


***Figure A-33.*** *Log-log plot of measured (blue) and simulated (red) pressure recovery and – derivative (green) versus equivalent time during the recovery period in section HLX11:2.*

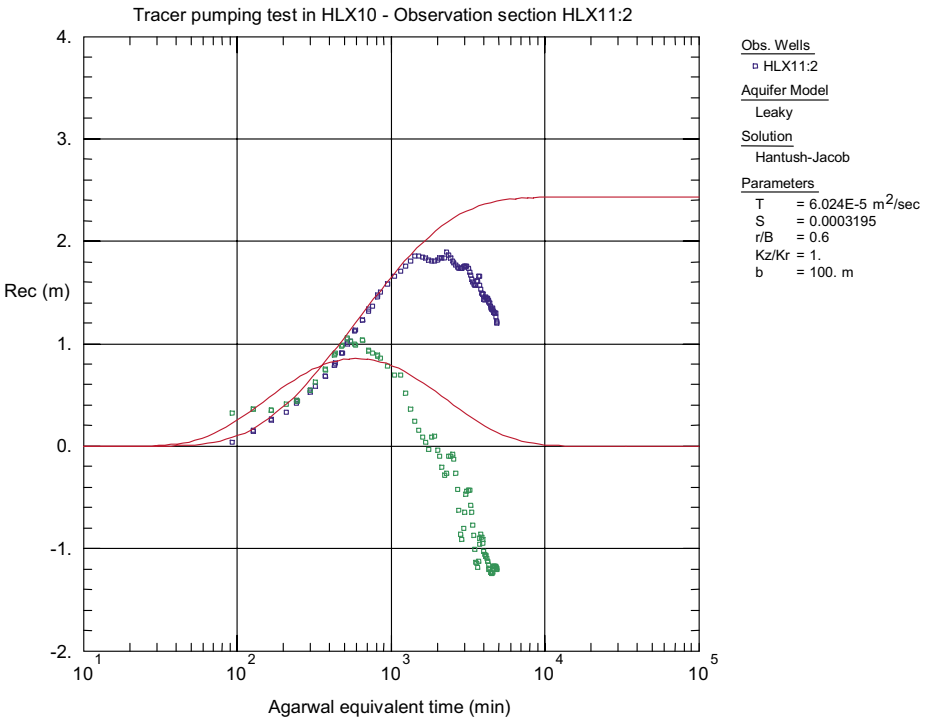


***Figure A-34.*** *Lin-log plot of measured (blue) and simulated (red) pressure recovery and – derivative (green) versus equivalent time during the recovery period in section HLX11:2.*